SISSA - SCUOLA
INTERNAZIONALE
SUPERIORE
DI STUDI AVANZATI
TRIESTE
Strada Costiera 11

ISAS - INTERNATIONAL SCHOOL FOR ADVANCED STUDIES

October 1985

ACTIVE GALACTIC NUCLEI

Thesis submitted for the degree

of

Master of Philosophy

CANDIDATE:

Piero Madau

SUPERVISOR:

M.A. Abramowicz

TRIESTE

CONTENTS

INTRODUCTION

The zoo of Active Galactic Nuclei (AGNs) includes quasars,Seyfert galaxies,radio galaxies and BL Lac objects. The evidence that all AGNs are very similar in fundamental ways is now overwhelming. A theoretical consensus concerning the nature of the common powerhouse seems to be forming,in the sense that accretion onto a supermassive,maybe spinning, black-hole is the basis of the great majority of recent models.

These "prime movers" are responsible for phenomena ranging in lengthscale from the giant radio sources ($\sim 10^{22}-10^{25}$ cm) through the narrow emission line regions ($\sim 10^{20}-10^{22}$ cm),compact radio sources ($\sim 10^{18}-10^{21}$ cm), broad emission line regions ($\sim 10^{17}-10^{18}$ cm), "thermal bumps" and non-thermal continua regions ($\sim 10^{14}-10^{17}$ cm),down to the shortest scales associated with occasional rapid X-ray variability ($\sim 10^{13}$ cm).

The most recent discovery about this activity is that it is often manifested in the production of jets of plasma that squirt out of the nucleus. Active nuclei are responsible for emission all the way from the lowest radio frequencies to the highest gamma-ray energies.

We will adopt the following operational definition :active galaxies are those which emit significantly more radiation in a given time than do the "normal" spiral,elliptical or irregular galaxies, and this predominantly non-thermal excess radiation appears to emerge from a very small region at the center of the galaxy. With this definition,AGNs constitute a heterogeneous class of objects. The brightest have bolometric luminosities that can exceed 10^{47} erg/s and at the other end of the scale it appears

that the central regions of most galaxies (including our own) display evidence for some form of non stellar emission. In this thesis we will not discuss the low power objects such as "liners" and "starbust nuclei" save to stress that their frequence of occurrence indicates that the majority of galactic nuclei have the potential to become active.

In the huge literature related to AGNs, two main lines of attack can be distinguished. One is to consider as fundamental the problem of energy generation and try to derive the main features of the emission spectrum associated with the different types of accretion flows. The thin disk,the radiation-supported and the ion-supported tori are different examples of this approach. The second line is to derive from the observations constraints on the radiation mechanisms and on the physical conditions in the emission region, which then may be found to favour one or another of the proposed central engines. Spectroscopy of the broad emission line region and the synchrotron self-Compton (SSC) model for the non-thermal emission are examples of the second approach. Both these lines will be followed in the thesis,with emphasis on some aspects of accretion models and on the SSC mechanism.

Chapter I consists of a summary of observations; quasars are discussed first, then BL Lacs,radio galaxies and Seyferts galaxies. Basic theoretical assumptions and arguments in favour of black-hole accretion models are examined in chapter II. Accretion flows characteristics are summarized in chapter III. The SSC mechanism is reviewed in chapter IV. This theoretical framework will then be applied in a detailed study of one of the most extraordinary active nuclei: the quasar 3C 273.

3C 273 has been observed at all frequencies from radio waves to gamma-rays. It is very well studied because it is the nearest

quasar (z=0.158) and intrinsically quite luminous. It exhibits remarkable features in all wavelengths ranges; it is a double radio sources with apparent superluminal motion; like other AGNs it shows jets, an outer jet at radio,optical and X-ray frequencies, and an inner jet (10 mas) detected with VLBI techniques; it emits strong UV radiation with a peculiar spectrum; the X-ray spectrum is very hard and it is,up to now,the only quasar identified as a high energy gamma-ray source.

Chapter V will be devoted to an overall interpretation of the spectrum of 3C 273. SSC model will also be applied in a statistical study of "Blazar" objects, and the distribution of Doppler factors derived for fourty objects.

The observational and theoretical literature on the subject of active nuclei is too extensive to be properly reviewed. More comprehensive recent reviews of some of the material contained below are to be found in Begelman, Blandford and Rees (1984), Rees (1984), Wiita (1985), Phinney (1983), Blandford (1984) and Begelman (1984).

CHAPTER I A FIELD GUIDE TO ACTIVE GALACTIC NUCLEI

I.1 QUASARS

The standard definition of quasars involves the following prime characteristics (Hazard 1979):

a) stellar appearance

b) a strong UV excess, due to a non-thermal optical continuum

c) variable optical emission

d) broad permitted emission lines (>3000 Km/s).

Roughly 10% of these optically selected QSOs are radio-loud (QSRs). The remaining 90% are radio-quiet and relatively weak X-ray sources (Zamorani et al. 1981). The infrared (10μm-2.2μm) spectra of most QSOs are roughly power-law, with spectral indices $<\alpha>\approx 1.2$, where the spectral index is defined in terms of the flux density and frequency as $F_\nu \propto \nu^{-\alpha}$.

In the near UV part of their spectra, most QSOs seem to depart, at least somewhat, from a smooth decline in F_ν versus ν. The "blue-bump" is a broad emission feature visible between 2,000 and 4,000 Å. Several theories have been proposed to explain this feature, among them a Balmer recombination continuum, blended Fe II lines and a two-photon continuum. The addition of a Balmer continuum to a background non-thermal power-law (with $\alpha \approx 1.1$) can explain much of the blue-bump, but an additional blackbody component -very possibly from an accretion disk- with temperature between 20,000 and 40,000 °K seems to be necessary in many objects (e.g. Shields 1978, Malkan and Sargent 1982). νI_ν seems to peak in the near UV; most of a QSO's total power output may thus be radiated in UV photons (see fig.1).

The radio emission from the QSRs typically comes from a compact (from 0.1" down to the limits of VLBI resolution, 0.0001"), flat-spectrum core and a steep-spectrum ($\alpha \approx 0.8$) extended (>10 Kpc) source. The spectrum of the radio-core has generally steepened by

30 Ghz as if to join smoothly onto the IR. The optical spectra of radio-loud and radio-quiet quasars are not very different. QSRs are also stronger X-ray sources than radio-quiet.

Little is known about the hard X-ray spectrum of QSRs. As stressed by many theorists (Fabian 1979,Lightman 1982),the high energy end of the spectrum is almost certainly most important in distinguishing among various emission mechanisms and particular models, since it is likely that the bulk of this emission is generated near the very center of the quasars or other AGNs. X-ray luminosities range from 10^{43} to 10^{47} erg/s.

Most (99%) QSOs have low optical polarization P<1%, with their electric vector stable and parallel to the axis defined by the extended radio-structure. They exhibit optical variability $\Delta I/I>0.5$ only on timescales of years or more (Stockman,Moore and Angel 1983). About 10% of QSRs are optically violent variables (OVVs), varying with $\Delta I/I \approx 5$ on timescales from months to days. These are almost invariably high polarized (P≈ 3-30%), radio-loud,dominated by a flat spectrum radio-core and with steep optical indices $\alpha > 1.5$ (Angel and Stockman 1981).

I.2 BL LACERTAE OBJECTS

BL Lacs have all the characteristics of OVV quasars (being infact grouped together under the name of "Blazar") except for the lack of emission lines, and thus redshifts, which makes it difficult to accurately measure their luminosities. Moreover,theoretical work suggests that they are not isotropic emitters (see chapter V),further complicating efforts to compute their intrinsic luminosities. The specific luminosity $\Omega/4\pi\,\nu I_\nu$ seems to peak in the far IR (see fig.1), ranging from 10^{44} to 10^{47} erg/s.

The radio emission is generally dominated by a flat spectrum radio-source but extended structures have been detected; radio spectra tend to remain optically thin up to about 90 Ghz, whereas quasars are usually optically thick above 10 Ghz. But,from those turnover frequencies up to the IR, both types of objects have $\alpha \approx 0.7$ (Landau et al. 1983). The high resolution maps of BL Lacs available from VLBI often show core-halo structures which support the hyphotesis that BL Lacs are an orientational rather than morfological class of AGNs,with jets oriented close to the line of sight; occasionally, clear jet features are found. The estimated linear sizes of these halos or jets (20-300 Kpc), the total radio powers (10^{41} -10^{44} erg/sec) and the spectral indices are all consistent with their being radio-lobes viewed end-on. A more detailed analysis of the relativistic beaming hyphotesis will be made in chapter V.

Perhaps the most outstanding feature of BL Lacs is their rapid variability in both intensity and polarization (Stein et al. 1976). The optical and IR radiation is highly polarized (5%<P<40%) and variable on timescales of days. Variations in the X-ray intensities are also seen on the same timescale. Since polarization measurements have been made at several frequencies, the Faraday rotation can be extracted; the average value of rotation is low ,implying a particle density $<10^{-3}$ cm^{-3}. Faraday rotation due to relativistic matter drops rapidly with increasing electrons Doppler factor γ ($\propto \ln\gamma / \gamma^2$); this means that either the plasma must be virtually devoid of electrons of energy >10 Mev or the emitting particles comprise equal densities of positrons and electrons.

A large,or even dominant, class of radio-quiet BL Lacs may exists. X-ray selected BL Lac candidates in fact show flatter spectra,lower radio to X-ray luminosity ratios than typical and could be

associated with misaligned jets (e.g. Maraschi et al. 1985). The overall spectrum of BL Lacs steepens substantially between radio and IR and between IR and UV frequencies, but not between UV and X-ray frequencies. The X-ray luminosities are relatively strong; the spectrum is usually steep ($\alpha \geqslant 1$) at energies $<$10Kev and lies well above the extrapolated UV flux, perhaps implying that the X-ray comes from inverse Compton scattering of photons off ultrarelativistic electrons. The spectrum at higher energies appears in many cases to be significantly flatter ($\alpha \leqslant 0.6$); a large fraction of the apparent bolometric luminosity may therefore be radiated in hard X-rays.

BL Lacs appear to be located in elliptical, rather than spiral galaxies.

I.3 RADIO GALAXIES

These are characterized by radio emitting structures which extend up to tens of thousands of kiloparsecs from the central galaxy (invariably an elliptical,rather than a spiral galaxy). The "classical doubles" were the first type recognized, with the two large radio-lobes nearly collinear with the central galaxy (core source).

It is now well established that beams of plasma -jets- propagate from galactic nuclei to energize the radio-lobes in the extremities. This idea was proposed well before radio jets were observed in any sources other than M 87 and 3C 273 (both have optical jets) and must be considered as one of the most successful fundamental predictions in recent astronomical history (Rees 1971, Blandford and Rees 1974). Jets are found more often in rather weak radio-sources and less often in the strong 3C sources and this could be due to the possibility that jets "waste" relatively more of the streaming energy in weaker sources.

Strong linear polarization ($P \approx 10\text{-}60\%$)is often seen along the longer jets with projected magnetic field mainly parallel to the jet near the origin, but further out often perpendicular to the jet axis (e.g. Miley 1980). Orientation of jets and lobes relative to the elliptic axis of the optical galaxy remains a matter of controversy despite many claims and counterclaims. Structures that are very much reminiscent of bent or swept-back jets characterizes the so-called "wide-angle tail" sources. Their jets seem to be physically distorted by the ram pressure of the intracluster medium through which the parent galaxy moves. Complex,twisting emission features are also seen, maybe resulting from ejection along an axis that is precessing.

The majority of radio-galaxies with small scale (<<1") nuclear

emission feature share some properties with the quasars: most have flat or inverted spectra interpreted as a result of the superposition of several components with different synchrotron self-absorption frequencies.

One of the most intriguing discoveries concerning compact cores is their frequently elongated jet-like structure, and the remarkable colinearity of those elongations with the extended jet. These milliarcsecond (mas) scale jets have now been realized to be quite common; a striking example is NGC 1275, where a closely aligned jet can be traced over six orders of magnitude in distance, from <1 pc to >1 Mpc (Begelman,Blandford and Rees 1984). A very important featureof the mas jets is their asymmetry; most of the time a single jet is fairly well aligned with an extend jet, but rarely are counterjets seen in the nuclei.

These effects probably result from relativistic motion nearly along the line of sight toward the observer; the apparent one-sidedness reflects the Doppler boosting of radiation from the approaching jet over that from the receding counterjet. This "Doppler favouritism" is particularly sensitive to orientation. The observed flux densities from the approaching and receding jets differ by a factor: $[(1+v_J \cos\phi/c)/(1-v_J \cos\phi/c)]$,where v_J is the jet velocity, α the spectral index and ϕ is the angle the jets make with the line of sight. A jet oriented at 10° to the line of sight with $\Gamma \approx 5$ would be brighter by a factor ~ 6000 than a similar counterjet,which would therefore be unobservable.

Galaxies at the center of high luminosity "classical doubles" sources sometimes show other evidence for nuclear activity, in the form of emission lines and nuclear X-ray sources. The nuclei of broad-line radio galaxies (BLRGs) have an optical continuum comparable to that of the surrounding galaxy; the nuclei of

narrow-line radio galaxies (NLRGs) are much fainter. Many radio sources,however, are associated with galaxies which are otherwise quite unremarkable and show no more evidence for nuclear activity than most "normal" galaxies.

1.4 SEYFERT GALAXIES

Seyferts are commonly divided into two classes, with the distinction based on spectra. The relative emission line widths are used to separate the Sey 1s,which have broad H lines but narrower forbidden lines, from Sey 2s,which have narrow H and forbidden lines.

The optical spectra of Sey 1s are essentially those of a QSO scaled down to be less luminous than its surrounding spiral galaxy. They are very weak flat spectrum radio sources; in contrast to BL Lacs, Sey 1s appear to have a remarkably standardized spectral shape. The spectrum flattens in the optical and near UV; the flattening is,like that in quasar spectra, well fitted by a superposition of a steeper power-law and a thermal bump peaking in the near UV which there contributes between 5 and 50% of the total flux (Malkan and Sargent 1982).

The optical to 2 Kev X-ray spectral index is quite steep ($\alpha_{ox} \simeq 1.3$), but above 2 Kev the spectrum flattens again, being well described by a power-law with universal spectral index $\alpha = 0.7 \pm 0.15$. Guilbert,Fabian and McCray (1983) have proposed to explain the optical spectra of Sey 1 broad line region with a two-phase model. Since Seyferts typically have flat X-ray spectra, high energy photons can produce additional Compton heating in infalling gas, and force a thermal instability. This produce a two-phase medium with clouds at 10^4 °K compressed by a hot medium with $T \sim 10^8$ °K. Since BL

Lacs have steeper X-ray spectra, this instability could explain their lack of emission lines.

The difficulty of subtracting the contribution of starlight makes measurements of the wavelength dependence of the optical polarization of Seyfert nuclei controversial (dust scattering implies wavelength-dependent polarization, contrary to electron scattering). Most Sey 1s are weakly polarized; Antonucci(1983)pointed out that, as for low polarization QSOs, the polarization electric vector is parallel to the direction of the radio emission, maybe indicating the existence of geometrically thin accretion disks in Sey 1 nuclei.

Compared to Sey 1s, Sey 2s are very weak soft X-ray sources. It is unclear what fraction of Sey 2s can be identified with a Sey 1 nucleus whose broad-line region and optical-UV continuum are obscured by dust and whose X-ray are absorbed by photoelectric absorption; the presence of the 10 μm silicate absorption feature strongly suggest that much of the far-IR emission is thermal radiation from dust. Sey 2s are about 10 times more luminous in the radio than Sey 1s. Most of the flux comes from an extended region , often having the appearance of a miniature double radio sources.

Like Sey 1s and QSOs, most sey 2s have low ($P<2\%$) optical polarization, but, in contrary to Sey 1s and QSOs, the optical vector is generally perpendicular to their radio source axis.

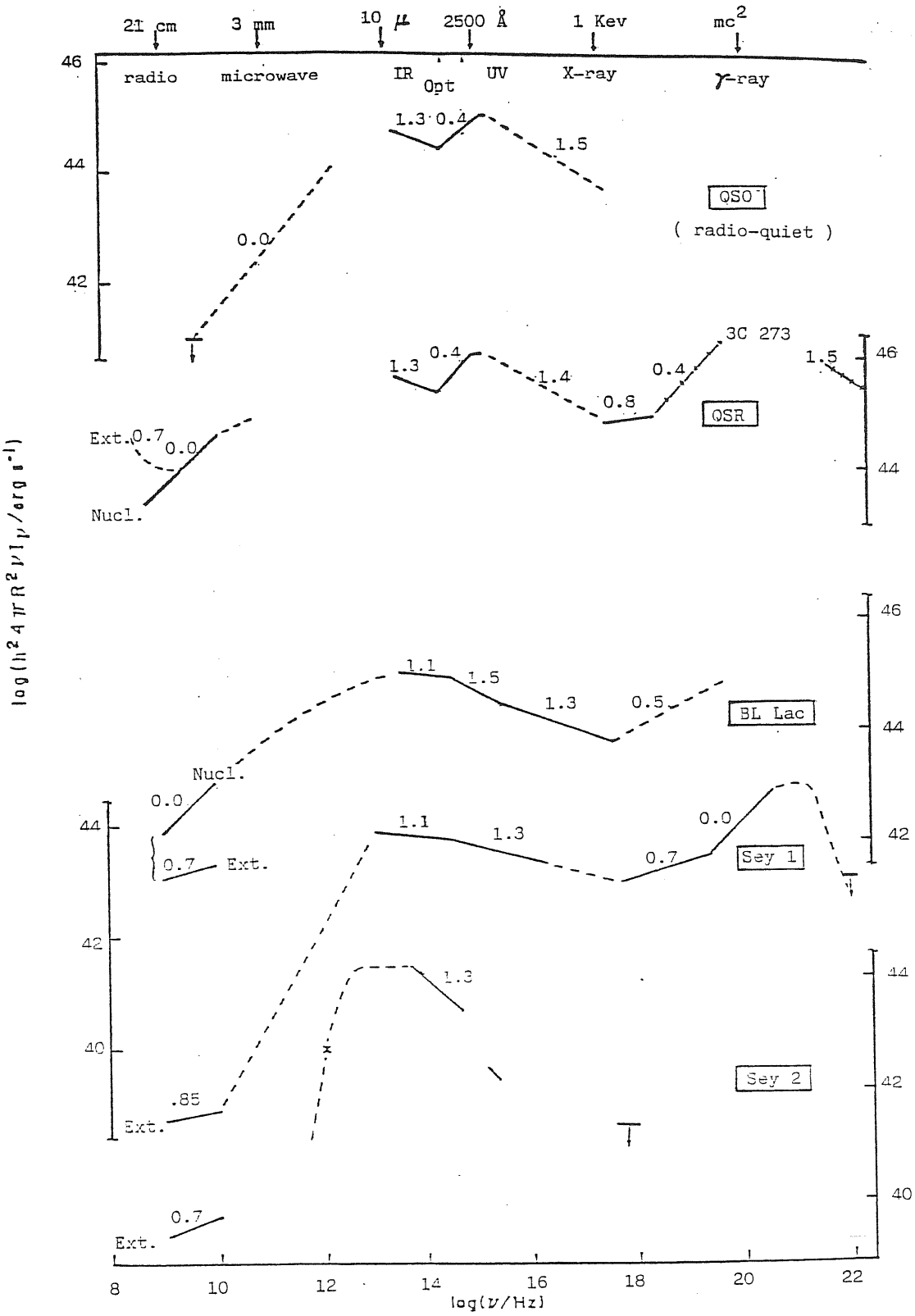

Figure 1: Representative energy spectra of the various classes of Active Galactic Nuclei. Numbers above the spectra give the local spectral index. (Adapted from Phinney, 1983)

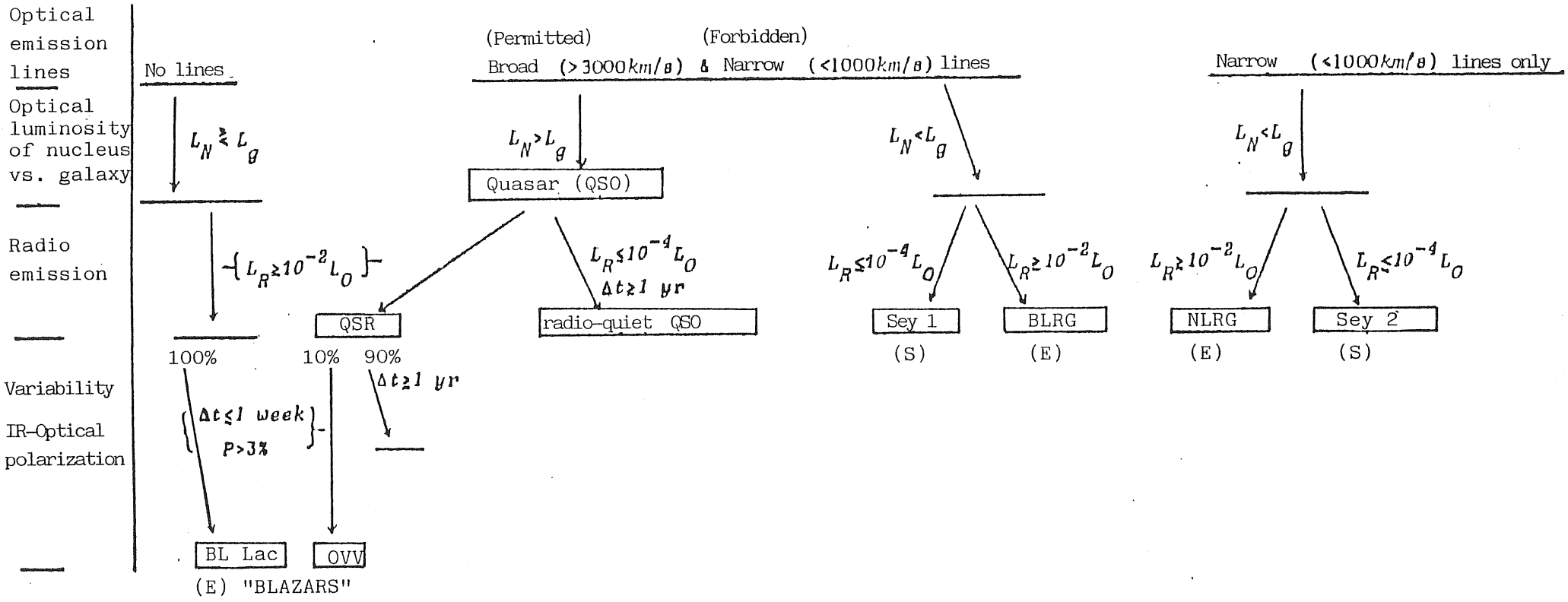

Figure 2: Classification of Active Galactic Nuclei. The percentage at the tails of the arrows are approximate branching ratios, where known. L_N and L_g are the optical luminosities of the active nucleus and its surrounding galaxy, respectively. L_R and L_O are the specific luminosities in the radio and optical bands. P is the percentage optical polarization. An (S) or (E) under a name means that the surrounding galaxy is almost invariably Spiral or Elliptical, respectively. (Adapted from Phinney, 1983)

CHAPTER II BASIC THEORETICAL INTERPRETATIONS

The preceding summary of observations has set the stage for our theoretical treatment of AGNs; in this section the stress will be placed on the physics and fundamental building blocks of active galaxies.

II.1 AGN LIFETIMES AND FUELING

Most current models assume that not all galaxies capable of evincing activity do so most of the time, so that their activity is sporadic. Statistical arguments can be used to estimate Seyfert galaxy lifetimes at $>10^8$ yr, since 1% of all spirals are Seyferts, and similar arguments imply that strong radio sources associated with giant elliptical galaxies could live up to 10^9 yr; indirect evidence (such as jet length) for quasars imply each active phase may be $\sim 10^6$ yr. Strong evidence for not terribly long quasar lifetimes is their statistical distribution in redshift; the space density of quasars at earlier times was in fact significantly greater than it is at present.

The most popular class of explanations for the AGN powerhouse involves accretion of gas onto a supermassive black-hole (SMBH) and detailed models of this nature will be discussed in chapter III. One significant problem for such models is the question of how enough gas can wend its way to the center of the nucleus where it can be accreted and where its gravitational energy can be liberated as radiation. Note that if a BH of mass $M_H=10^8$ $M_\odot$ radiates near its Eddington limit (see III.1) with an efficiency of mass-to-energy conversion of η, then the accretion rate must be equal:

$$M_H \approx (0.1\ M_\odot/yr)\ L/L_E\ \eta^{-1} \quad .$$

Several processes have been proposed to solve this problem, among them genuine stellar collisions, tidal disruption and partial swallowing of stars by the central BH (Hills 1975) and mass loss from O and B stars, either by normal winds or by X-ray induced stellar winds (Shields and Wheeler 1978). However,the tidal process becomes less efficient for bigger central BHs,since the tidal disruption radius r_T grows less quickly than the gravitational radius r_G ($r_G \propto M_H$, $r_T \propto M_H^{1/3}$). To avoid demanding the very high stellar densities in the nuclear region that may be necessary in order to supply a constant accretion rate $1M_\odot$/yr, it has been suggested that active nuclei could store gas, perhaps in a disk,for relatively long quiescent periods. An instability could then release this matter, and allow a high accretion rate for a shorter time. All these processes may be important in different galactic nuclei or at different times within the same nucleus.

A closely related question involves asking if interactions between galaxies can trigger the observed activity; some recent observations indicate that active galaxies of all types show evidence of stimulation by nearby galaxies (Balick and Heckman 1982). Over 30% of a sample of 45 quasars with $z<0.62$ seem to be currently interacting; this is consistent with the idea that QSOs flare up after receiving material from a galaxy that mergers with it or passes close by (Hutchings and Campbell 1983). More recently, Gaskell (1985) has proposed that it is not actually the detected neighburing galaxy that is stimulating quasar activity, but instead a direct collision with one of the several unseen dwarf satellite galaxies in the system.

II.2 SOME ARGUMENTS IN FAVOUR OF BLACK-HOLES

Short term variations in luminosity provide the best upper limits for the sizes of AGN active regions. In the absence of special geometries and relativistic motions, the causality argument implies that significant variations over a time t implies a source no larger than: $\Delta R < c \Delta t$.

The radius of the event-horizon of a BH of mass M_H with angular momentum parameter a is:

$$r_H = 1.48 \times 10^5 \ (1+\sqrt{1-a^2}\ ) \ (M_H/M_\odot) \ \text{cm}$$

and it provides the minimum possible time over which such variations are conceivable for BH models. Periodic variations are further constrained by feasible rotational timescales in accreting material; a common way of explaining short-lived periodic variations is to assume that the acctreting disk contains a "hot-spot" or active region which is spiralling into the central BH. For a Schwarschild hole, thin keplerian acretion disks have their innermost stable orbit at $6GM_H/c^2$, and thick pressure-supported disks reduce this value to $4GM_H/c^2$ (e.g. Abramowicz, Jaroszynski and Sikora 1978); for an extreme Kerr-hole (a=1), both the innermost bound and stable orbits coincide at $r_H = GM_H/c^2$. Thus a periodic variation could exists down to timescales of about:

$$P = 2\pi \ r_H/c \approx 3 \times 10^{-5} \ (M/M_\odot) \ \text{sec}$$

Variations on timescales less than these either preclude BH models of a given mass or demand relativistic bulk motions. Several groups have recently reported tentative detections of ~ 15 min radio periodicity in the BL Lac object OJ 287 (e.g. Carrasco, Dultain-Hacyan and Cruz-Gonzales 1984) which is consistent with $M_H < 3 \times 10^7 M_\odot$. They pointed out that a mass this low would give

$L/L_E \gg 1$ for OJ 287, a further indication that relativistic beaming is important for these objects.

These insights can be further constrained with the assumption that the luminosity of an accreting BH cannot exceeds the Eddington limit $L_E = 4\pi\, cGM_H / K_T$ (Elliot-Shapiro 1974) to get:

$$\log \Delta t_{min} > \log L - 43.$$

An updated version of this relation (Abramowicz and Nobili 1982) takes into account the fact that radiation-supported tori allow for apparent luminosities greater than L_E by a factor $\sim$ 50-100 (Sikora 1981). The latest compendium of over 60 AGNs (Bassani, Dean and Sembay 1983) indicates that three BL Lacs may be in conflict with even highly anisotropic emission unless relativistic beaming is assumed (fig.3).

If one assumes that an outburst is produced by material that is at least partially opaque due to electron scattering, then the light travel time across the emission region is boosted to become:

$$\Delta t \geq \Delta r/c\ (1+\tau_{es}) \qquad 2.1$$

A general constraint exists on the amount of energy associated with the conversion of mass M :

$$\Delta L\, \Delta t = \eta Mc^2 \sim \eta n \Delta r^3 \qquad 2.2$$

where n is the density. From (2.2) we write :

$$\Delta r \sim (\Delta L\, \Delta t/\tau_{es})^{1/2} \quad \text{and, using the eq.(2.1):}$$

$$\Delta t \sim (1+\tau_{es})^2 /\tau_{es}.$$

One minimizes Δt when the source has a radius such that $\tau_{es} = 1$, so that we get (Fabian and Rees 1979):

$$\Delta L \lesssim 2 \times 10^{42} \eta \, \Delta t \quad \text{erg/s.}$$

This general limit is probably violated by at least a few BL Lacs and OVVs with $\Delta t < 10^4$ sec and $\Delta L > 10^{46}$ erg/s, since η cannot excceds unity. However, relativistic flow toward the observer again comes to the rescue. So the SMBH accretion picture remains consistent with all evidence involving time variability; but it is also clear that Doppler effect and significant anisotropies are indicated by some of the observations.

Evidence that a great deal of mass is squeezed within very small volumes in galactic nuclei is growing, and lends additional support to the SMBH hyphotesis. In general, surface photometry of elliptical galaxies shows a smooth, quasi-isothermal stellar distribution. The presence of a point-mass would tend to distort the latter, introducing a cusp into the light distribution (e.g. Shapiro and Lightman 1976); moreover, the presence of an extra " r^{-1} " deep potential well will cause a rapid rise in the velocity dispersion.

M 87 (Virgo A) shows direct evidence for a supermassive central condensation through both light cusp and velocity dispersion, with $M_H = 2.6 \times 10^9 M_\odot$ (Young et al. 1978). In the Galactic centre too, considerable recent evidences point to a massive central BH. Both mass distribution (Crawford et al. 1985) and velocity field investigations by [Ne II] emission lines (Serabyn and Lacy 1985) seem to indicate a central condensation with $M_H \sim 4 \times 10^6 M_\odot$. Moreover, the size of the Galactic centre compact radio-souce has been recently resolved to be < 20 AU $= 3. \times 10^{14}$ cm, again pointing to an extremely compact source (Lo et al. 1985).

The idea that is almost impossible for a galaxy with a strong central condensation to avoid producing a SMBH is now a popular one (e.g. Rees 1984 and, for recent numerical simulations Shapiro and

Teukolski 1985). Fig.4 indicates schematically the various evolutionary pathways that may be involved in the accumulation of gas and stars in the gravitational potential well at the center of a galaxy. The important message -the bottom-line - is that the most likely endpoint of dense star clusters or supermassive stars will be the collapse of a large fraction of the mass involved to a massive BH. Furthermore,a black-hole embedded in infalling matter offers a more efficient power-source that any conceivable progenitor.

To summarize,it is fair to say that theoretical arguments,coupled with observational evidences in favour of compact,massive objects and accretion mechanisms, lead to the conclusion that SMBHs are the most probable candidates at the core of the AGN phenomena.

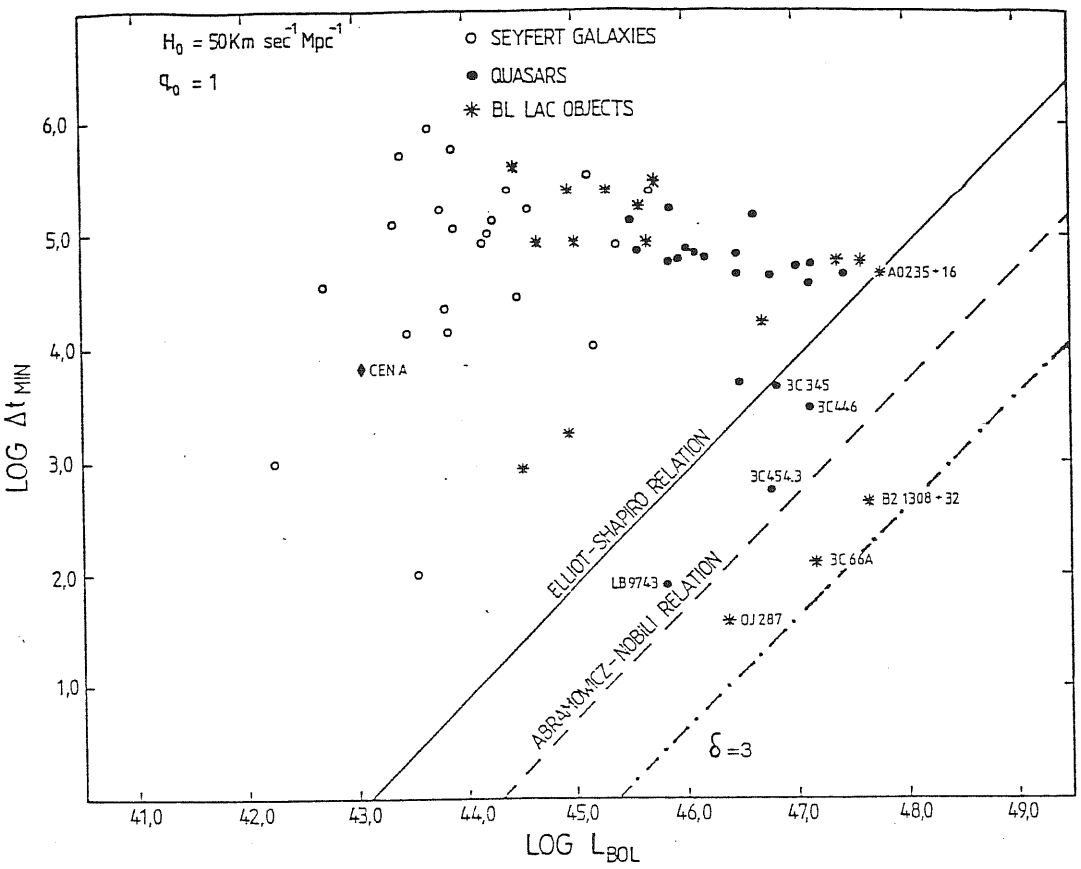

Figure 3: The minimum variability timescale is plotted against the bolometric luminosity for a selection of AGNs. A mildly relativistic beaming factor of δ = 3 is enough to reconcile the observations with black-hole models. (Adapted from Bassani,Dean & Sembay 1983)

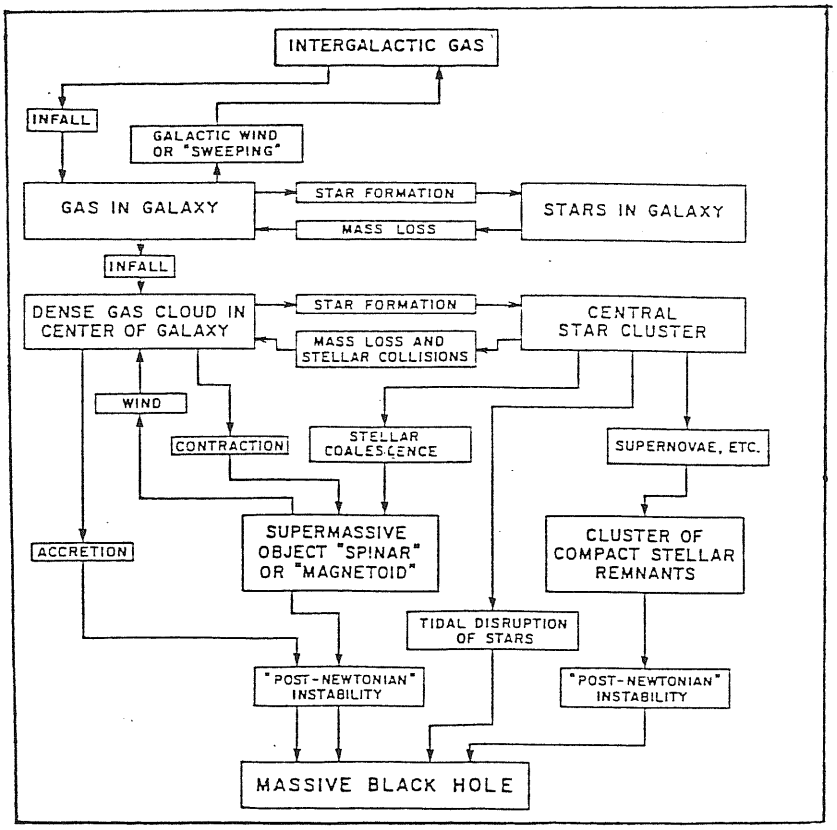

Figure 4: Flow diagram indicating the various processes whereby gas and stars accumulate at the center of a galaxy. The final result is likely to be the formation of a massive B.H. (from Begelman,Blandford & Rees 1984).

CHAPTER III. ACCRETION FLOWS

The details of the accretion flows and energy generation are the subject of much current research and tremendous debate. This chapter is devoted to a brief presentation of BH accretion mechanisms.

III.1 SOME FIDUCIAL NUMBERS

Before focusing on specific properties of accretion flows, it may be helpful at this stage to introduce some characteristic quantities, which give a feel for the orders of magnitude involved and for what approximations are justified.

A central mass M_H has a gravitational radius:

$$r_g = 2GM_H/c^2 \approx 3\times10^{13}\ M_8\ \text{cm},$$

where M_8 is the mass in units of $10^8\ M_\odot$. The characteristic minimum time for variability is:

$$t_{dy} = r_g/c \approx 10^3\ M_8\ \text{sec}.$$

A characteristic luminosity is the "Eddington limit" at which radiation pressure on free electrons balances gravity:

$$L_E = 4\pi\, cGM_H m_p c/\sigma_T \approx 1.3\times10^{46}\ M_8\ \text{erg/s}.$$

Related to this is a characteristic timescale:

$$t_E = \sigma_T\, c/(4\pi\, Gm_p) \approx 4.\times10^8\ \text{yr}.$$

This is the time it would take an object to radiate its entire rest-mass if its luminosity were L_E .

The characteristic blackbody temperature if the luminosity L_E

emerges from a sphere of radius r_g is:

$$T_E \approx 4.\times10^{5}\ M_8^{-1/4}\ ^\circ K,$$

thus thermal radiation from optically thick material would be in the far UV. Note that KT_E is far below the "virial temperature" $KT_{vir} \approx m_p c^2 r_g / r$; gas that has cooled down to thermal equilibrium at a temperature $\sim T_E$ can therefore only be supported against gravity if radiation pressure exceeds gas pressure by a large factor $\sim T_{vir} / T_E$.

We can now define a characteristic radiation pressure:

$$p_E = 1/3\ aT_E^4 \approx 6.\times10^{7}\ M_8^{-1}\ \text{dyne/cm}\ ,$$

density:

$$n_E = 3p_E / (m_p c^2) \approx 10^{11}\ M_8^{-1}\ \text{cm}^{-3},$$

and equipartition magnetic field:

$$B_E = \sqrt{8\pi p_E} = 4.\times10^{4}\ M_8^{-1/2}\ \text{G}$$

The synchrotron lifetime for a relativistic electron in the field B_E is:

$$t_{SE} = 8.\times10^{8}\ B_E^{-2}\ \gamma^{-1} \approx m_e/m_p\ \gamma^{-1}\ r_g/r \approx \gamma^{-1}\ M_8\ \text{sec}$$

and it is $<< r_g/c$ so, in any model involving such mechanism, the radiating particle must be injected or repeatedly reaccelerated "in situ".

III.2 MODES OF ACCRETION

The way in which gas flows into an accreting object depends largely on the conditions where it is injected. If the gas has no angular momentum, it can flows in radially. However, spherical accretion is probably of limited relevance to the observations

simply because it is hard to see how infalling gas can have so little angular momentum to move radially near the event-horizon of the hole . Besides,the observations indicate that all classes of active nuclei exhibit strongly aspherical radio-structures,such as jets. For these reasons,coupled with the low efficiency of mass-to-energy conversion (if magnetic fields or turbulence are not invoked) and the lack of any fiducial length scale to fix the rapid variability often seen (shocks?), we will confine our attention to accretion with angular momentum, which can single out the direction in space, if not necessarily produce the jets themselves.

The flow pattern completely changes if the inflowing gas has a small amount of angular momentum. The quasi-spherical approximation breaks down when $l^2(r) > GM_H r$,where $l(r)$ is the specific angular momentum per unit mass. If the inflowing gas is injected more or less isotropically from large r but has angular momentum such that $l > l_{ms} = \sqrt{3}\, r_g c$ (where l_{ms} is the specific angular momentum at the innermost stable circular orbit), then the gas must give up some of its angular momentum via viscous torques before it can cross the event-horizon.

In the process it dissipates a certain amount of binding energy,which may be either radiated away or retained by the gas in the form of heat. An accretion flow which is able to radiate away most of its binding energy forms a thin accretion disk. Thin disks have been studied extensively in connection with cataclysmic variables and X-ray binaries (see Pringle 1981 for a rewiew) but we don't know whether such systems can be scaled up to account for activity in AGNs, essentially because we don't understand some of the physic involved (e.g. viscosity mechanism and the role of non-thermal emission processes). Radiation pressure and electron scattering play important roles in disks and the structure of such

disks is largely governed by the ratio of the actual accretion rate to the Eddington accretion rate: $\dot{M}_E = L_E / c^2$.

If $\dot{m} = \dot{M}/\dot{M}_E < 1$, then the bulk of the emission comes from a region only $\sim 5 r_g$ in size and the physical conditions can be scaled in terms of the fiducial quantities defined below. It can in fact be shown that, at a distance r from the hole, these characteristic quantities are:

$t_{IN} \sim (r_g / r)^{-3/2} \; v_K / v_{IN} \; t_{dy}$; inflow time

$n_{IN} \sim \dot{m} \; (r_g / r)^{3/2} \; v_K / v_{IN} \; n_E$; particle density

$\tau_{es} \sim \dot{m} \; (r_g / r)^{-1/2} \; v_K / v_{IN}$; optical depth to electron scattering,

where the subscript k stands for keplerian and the ratio v_K / v_{IN} depends on effective viscosity.

If this ratio is fixed, then flows with similar values of $\dot{m}$ should be qualitatively similar. In particular, accretion rate $\dot{M}$, timescale t_{dy} and length scale r should all scale with M_H for similar disks. Thus, the characteristic density in a disk scale as $\rho \propto \dot{M} t / r^3 \propto \dot{m} / M_H$. The cooling timescale is inversely proportional to density, so the ratio $t_{cool} / t_{dy} \propto 1/\dot{m}$ and is independent of M_H. In other words, an accretion flow may not be able to cool and form a thin disk if $\dot{m}$ is too small. Such a flow may instead puff up to form an ion torus supported by gas pressure (Rees et al. 1982).

Alternatively, consider a flow with very large $\dot{m}$. The electron scattering optical depth scales as $\tau_{es} \propto \rho r \propto \dot{m}$. This is also proportional to the ratio of photon diffusion time to dynamical time, so radiation is unable to leak out of a flow with $\dot{m}$ too large. Such a flow forms a radiation torus supported by radiation pressure. Because the luminosity required to inflate the torus is $> L_E$, such structure may form whenever $\dot{m} >> 1$ (e.g. Abramowicz, Calvani and

Nobili 1980).

We can define the three main accretion modes starting from a different point of view. The virial temperature is given by :

$$KT_{VIR} = GMm_p/r = 1/2\ m_p c^2\ (r_G/r);$$

the "transrelativistic region" can be defined as that where KT_{VIR} has to exceed $m_e c^2$;it corresponds to radii $r<10^3 r_G$. In general,Compton (and other) cooling processes will maintain $KT_e < m_e c^2$. So pressure gradients cannot balance gravity in the transrelativistic region unless either:

i) radiation pressure balances gravity,which requires $L \approx L_E$ or $\dot{m}>1$ (radiation torus);

ii) ion pressure balances gravity (ion torus). This requires $T_{ION} \approx T_{VIR}$ ($>>T_e$),that is to say ions are decoupled from electrons; this is possible if the electron-ion energy transfer is slow, i.e. $t_{ION-e^-} > t_{IN}$. This in turn requires low densities and the absence of collective plasma effects coupling the two species, which again requires (Rees et al. 1982): $\dot{m} < 50\ (v_{IN}/v_K)^2$.

If neither i) or ii) is fulfilled,then the material at $r<10^3 r_G$ must be either in almost free-fall, or in a rotationally supported thin disk.

TABLE 1

MODES OF ACCRETION

	THIN DISK	RADIATION TORUS	ION TORUS
Accretion rate $\dot{M}$	$< \dot{M}_E$	$> \dot{M}_E$	$< 50\ (v_{inf}/v_{kepl})^2\ \dot{M}_E$
$\frac{t_{thermal}}{t_{dynam.}}$	≈ 1	$\gg 1$	$\gg 1$
Radiative efficiency	~ 0.1	$\sim 0.01\ (\dot{m}^{-1})$	$\ll 1$
Basic input radiation	Thermal (Comptonized) Bremsstrahlung	Thermal (Comptonized) Bremsstrahlung	Non-thermal (Synchrotron + Compton)
Basic radiation output	Optical+UV	Optical+UV	IR-synchrotron + IC gamma-rays
$\frac{\text{Non-thermal}}{\text{thermal}}$	< 1	< 1	High
Nice features	Corona?	Funnel, radiation pressure-driven jets, winds	Funnel, exotic MHD jets? $T_i = m_p/m_e\ T_e$

III.3 THE THERMAL BUMP

The generic properties of the three main modes of accretion are summarized in table 1. One obvious difference between them is in the quality of the spectra they produce. Thin disks and radiation tori are primarily thermal emitters, with spectra peaking in the UV. Either of them seem capable of producing a power-law continuum; the most likely loci for non-thermal emission are a hot-corona above the disk photosphere and relativistic jet driven by radiation in the funnel of radiation tori.

The decomposition of quasars and Seyferts spectra into a thermal UV bump and a non-thermal component by Malkan and Sargent (1982) and Malkan (1983) does not by itself discriminates between the two models. Specifically, thin disks are broad band emitters,with a flat and smooth spectrum built up from emission at a range of temperatures. The integrated spectrum of a radiation torus cannot be predicted with such theoretical certainty and its "doughnut" shape forces a new parameter to enter in the game: the angle between the rotation axis and the line of sight (viewing angle) which account for self-shadowing effects. In particular,the surface temperature distribution of the torus is such that,at large viewing angle, the observed spectrum will resemble a cool blackbody spectrum (see fig.5,6).

Malkan (1983) has fitted his data for six luminous quasars to both thin disks and blackbody spectra, and prefers the broad band model because of the flatness in the thermal component just shortward of the Balmer continuum. Blandford (1984),however,replotted some of Malkan's published data in terms of νF_ν vs ν (fig.7) revealing a well defined hump that looks very much like a single-temperature blackbody at T~27,500°K. Both results are sensitive to the assumed spectrum of the non-thermal continuum,but it is curious that all of

Malkan's QSOs can be fitted by single-temperature blackbodies in the range 25,000-30,000 °K. New important observations have been recently presented by Lawrence and Elvis (1985).The quasar PG 1211+143 shows a large excess at soft X-ray energies (fig.8) that could be connected with the UV-bump, both representing the two ends of a single,highly luminous excess with $T_{BB} \approx 10^6$ °K ;such temperature can be expected from the very inner region of accretion disks. In the framework of radiation tori model ,PG 1211+143 would be an object seen almost along the funnel axis.

Polarization may be a further discriminant between radiation tori and thin disks; we expect disks to exhibit a higher degree of polarization -at least a few percent due to electron scattering (Angel 1969)- that nearly spherical tori, a feature which is not seen in QSOs (Angel and Stockman 1980). A second difference between the modes of accretion is in the radiative efficiency of the flow. For example,the weakness of the radiation from the nuclei of many radio-galaxies,compared with the inferred kinetic energy fluxes into the jets and lobes ($L_{NUCL}/L_{JET} \sim 10^{-4}$), support the ion torus as the dominant mode of accretion in these objets.

The dimensionless quantity $\dot{m}$ is,as we have seen,the most important parameter in determining the modes of accretion flows,so the question is now whether observations do provide some independent means of determining $\dot{m}$ (or,with a fixed η ,determining M_H) in a given object.

For QSOs and Sey 1s the best quantitative diagnostics are supplied by the broad emission lines which show remarkably similar characteristics (as velocity dispersion,ionization parameter,covering factor) over a wide range of luminosities. Unfortunately,we don't know at present whether the velocity dispersions σ_{BLR} of the broad emission lines ($3,000 < \sigma_{BLR} < 20,000$ Km/s)

are keplerian velocities or substantially exceed v_K (in principle the flow pattern could be deduced by monitoring variations in the line-profile, e.g. Ulrich et al. 1984).

However, two clear-cut possibilities can be inferred if we write the keplerian velocities as (Begelman 1984):

$$v_K\ (BLR) \sim 900\ (L_E/L_{UV})^{1/2}\ (L_{UV}/10^{46}\ erg/s)^{1/4}\ (n_e/10^{10}\ cm^{-3})^{1/4} \Xi^{1/4}\ Km/s,$$

where L_{UV} is the luminosity of the ionizing continuum, n_e is the density of the line emitting gas and Ξ is the ionizing parameter ~0.1-1. Now, if $\sigma_{BLR} \sim v_K$, then quasars and Sey 1s must be substantially sub-Eddington, with $\dot{m} \ll 1$. The appearance of the thermal component in the spectrum then argues for a thin disk model. If QSOs are all very sub-Eddington, then there must be some 10^{10} $M_\odot$ BH lurking in the most powerful ones (Wandel, 1985).

If, on the other hand, it can be shown that the line emitting clouds substantially exceed the local escape speed (e.g. they are swept out in a radiation driven wind), then L is much closer to or exceeds L_E. At least, we don't expect σ_{BLR} to be smaller than v_K; this places a lower limit on $\dot{m}$ in the range 10^{-2} - 10^{-3}.

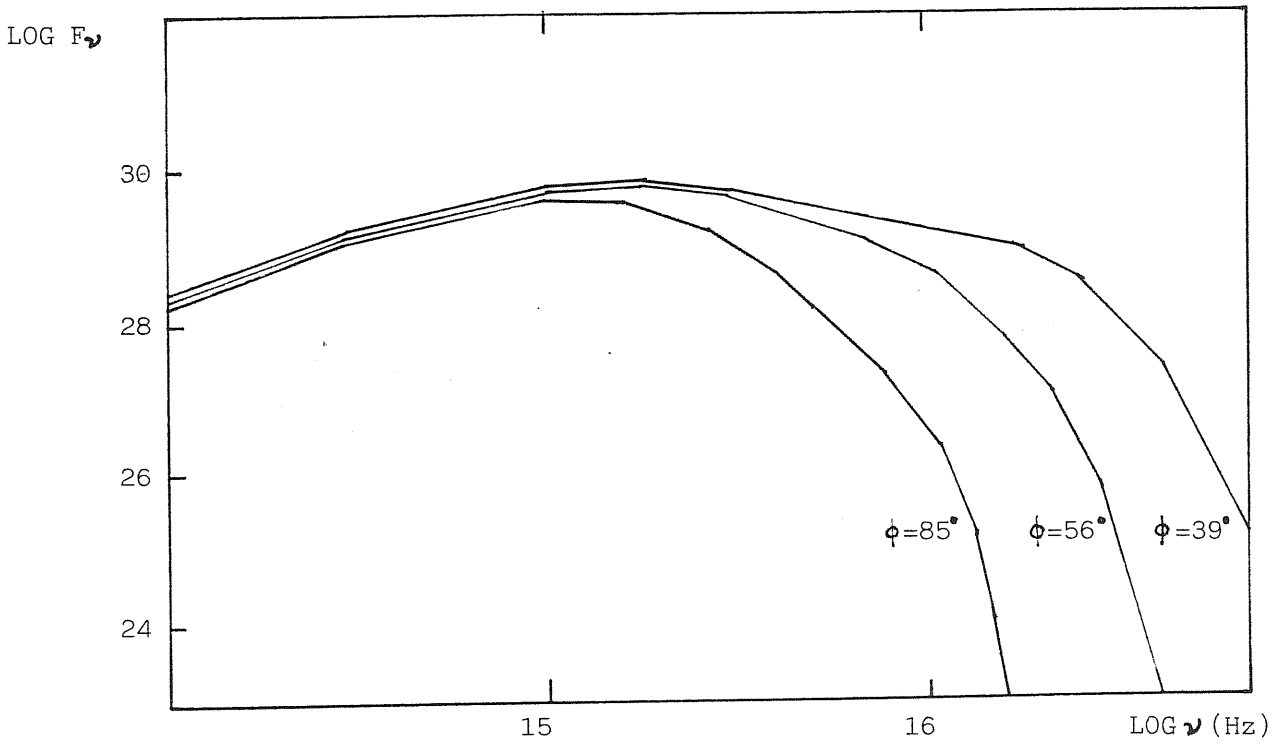

Fig. 5

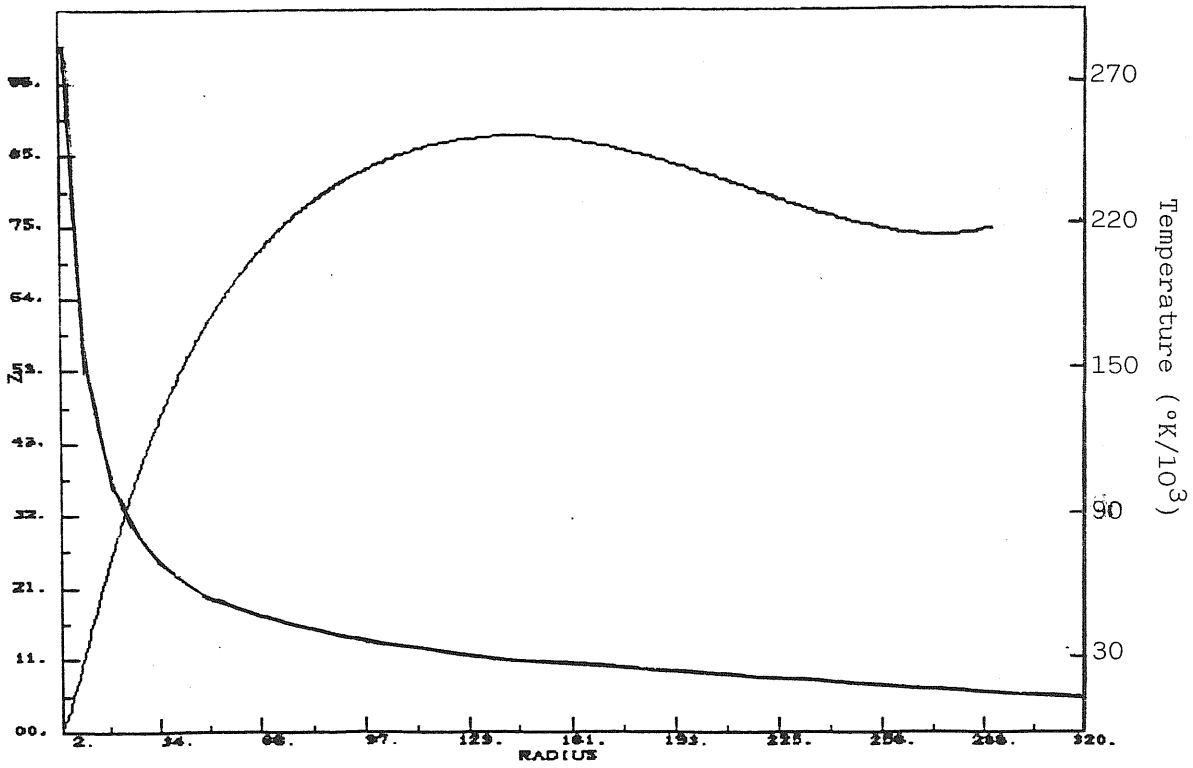

Fig. 6

Fig.5: Thermal spectra of a thick accretion disk at various viewing angles . The $\phi = 85^\circ$ spectrum is close to a single temperature blackbody one.

Fig.6: Shape and temperature distribution of a thick accretion disk. The mass of the hole is 10^8 $M_\odot$ and the angular momentum distribution $l(r)=l_{in} + A\ (r - r_{in})$, with $r_{in}=2$

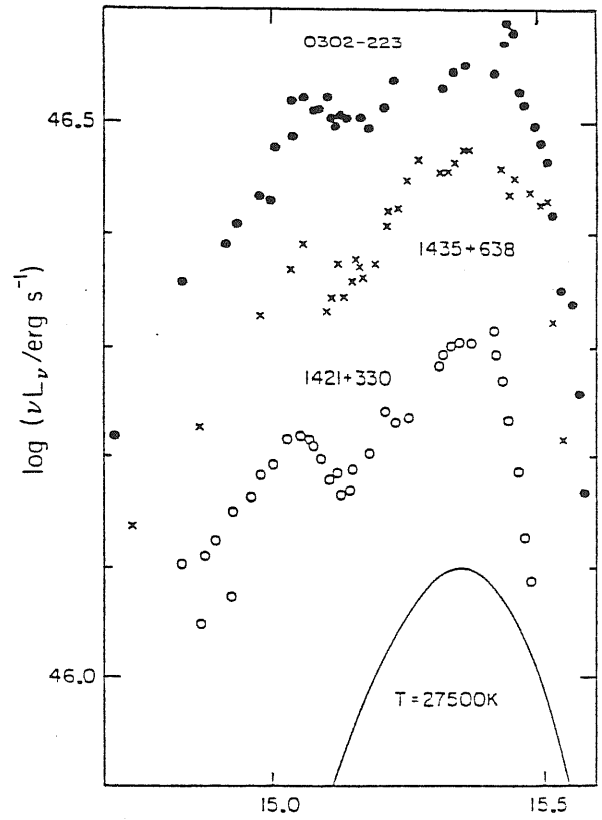

Fig. 7

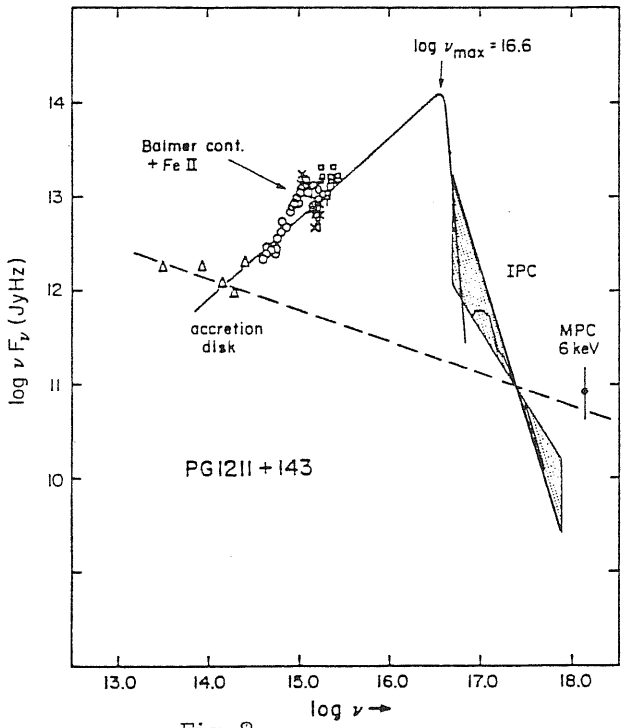

Fig. 8

Fig.7: 3 quasar spectra from the data presented by Malkan (1983) in terms of luminosity per logarithmic frequency interval. For comparison a blackbody spectrum with T=27,500°K is also exhibited (Blandford 1984).

Fig.8: A $\log \nu E_\nu$ vs. $\log \nu$ plot for PG 1211+143. An example of an optically thick,geo - metrically thin accretion disk spectrum is shown (Elvis 1985).

CHAPTER IV. NON-THERMAL EMISSION MODELS

Although non-thermal processes play a role in all AGNs,we will discuss here primarily quasars and BL Lac objects;in these objects the non-thermal continuum is most pronounced. In particular, OVV quasars and BL Lacs (Blazars) are characterized by the optical properies of rapid variability,high polarization and steep spectra which suggest electron synchrotron as the mechanism for the radio emission.

The size of the emitting region,either inferred by time variability or by VLBI, is typically $\sim 10^{17}$ cm,which requires a high radiation energy density as compared to the energy density of the magnetic field. This suggests that the inverse-Compton scattering (IC) would be a primary and catastrophic electron energy loss mechanism. The intensity of the IC X-ray emission in such a scenario has been predicted by Jones,O'Dell and Stein (1974). In many cases,the observed X-ray fluxes are much lower than those predictions,suggesting that the naive SSC theory is not sufficient.

One explanation of this discrepancy (e.g. Blandford and Konigl 1978) invokes the beaming of the radiation due to relativistic bulk motion. In this scenario an ejection of emitting matter towards the observer may cause an enhancement of the source brightness; the excess of predicted flux density over observed is thus believed to be due to relativistic bulk motion. An excess of observed over predicted leads to no special conclusion.

IV.1 SYNCHROTRON SELF-COMPTON

In this process, ultrarelativistic electrons of energy $\gamma m_e c^2$ are accelerated in a magnetostatic field B (e.g. Rybicki and

Lightman 1979). Individual electrons orbit about the field with frequency ν_L/γ (where $\nu_L = eB_\perp/(2\pi m_e c^2)$ is the Larmor frequency), radiating a total power given by the relativistic Larmor formula:

$$P_s = 4/3\,\gamma^2 \sigma_T\, cB^2/8\pi \quad , \qquad 4.1$$

where σ_T is the Thomson cross-section and we averaged over an isotropic distribution of electrons. We can define an electron cooling time:

$$t_s = \gamma m_e c^2 / P_s = 8\times10^{8}\, B^{-2}\, \gamma^{-1} \text{ sec.} \qquad 4.2$$

An ultrarelativistic electron radiates high armonics of the gyrofrequency. The characteristic radiated frequency ν_c can be estimated as follow: relativistic aberration gives a beam pattern for an individual electron of angular width $\sim \gamma^{-1}$, and so radiation is emitted in the direction of an observer lying in the orbital plane for a time $\delta t_{em} \sim 1/\nu_L$.

The pulse seen by the observer, however, due to Doppler effect, has duration : $\delta t_{ob} = \delta t_{em}(1-v/c) \approx \delta t_{em}\,\gamma^{-2}$, and so $\nu_c \sim \gamma^2 \nu_L$.

Radio-spectra are usually power-laws with the spectral flux F_ν conventionally measured in janskys (1 Jy=10^{-23} erg/s/cm /Hz). If the electron energy distribution function satisfies : $dN(\gamma)/d\gamma = k\gamma^{-p}$, then:

$$F_\nu \propto \int k\gamma^{-p} P_s\, \delta(\nu-\nu_c)\, d\gamma \propto kB^{1+\alpha}\, \nu^{-\alpha} \quad , \qquad 4.3$$

where α, the spectral index, is given by: $\alpha = (p-1)/2$.

Synchrotron radiation is linearly polarized perpendicularly to the magnetic field; the maximum degree of polarization, corresponding to a uniform field, is P=70% .The brightness temperature $T_b = c^2 I_\nu / 2\nu^2 K$ of a synchrotron source is limited by the kinetic temperature of the

emitting electrons, i.e. $T_b < \gamma m_e c^2/3K$. The flux observed from an optically thick synchrotron source then satisfies : $F_\nu \propto \nu^2 T_b \propto \nu^{2.5}$.

Photons are scattered by free electrons with the Thomson cross-section σ_T, for frequencies in the rest-frame $\nu < m_e c^2/h$. At higher frequencies, the Klein-Nishina formula in the ultrarelativistic regime can be approximate by:

$$\sigma = \sigma_T \left[\frac{3 m_e c^2}{8 h\nu}\right]\left[2 \ln\left(\frac{h\nu}{m_e c^2}\right)^{1/2}\right]$$

(Blumenthal and Gould 1970). Photons that are more energetic that the scattering electrons will, on balance, lose energy due to Compton recoil by an amount $\Delta\nu/\nu \sim h\nu/m_e c^2$ each scattering.

Alternatively, when the electrons are hotter, the photons will be scattered to higher energies. Individual scatterings will Doppler-shift photon frequencies up or down by an amount $\Delta\nu/\nu \sim (KT/m_e c^2)^{1/2}$ However, blueshifts (approaching collisions) outweight redshifts (receding collisions) by an amount also $\sim (KT/m_e c^2)^{1/2}$, implying a net Compton cooling of the electrons.

Compton cooling of relativistic electrons is known as the inverse Compton effect. In the rest frame of the electron, most incoming photons appear to have a frequency $\sim \gamma\nu$. Provided that this does not exceeds $m_e c^2/h$, the photons will be scattered elastically. Lorentz transforming back to the original frame gives a net average boosted frequency $\sim \gamma^2\nu$ (assuming a complete isotropy). Since the intermediate photon energy can be as high as, say, 100 Kev and still be in the Thomson limit, it can be seen that photons of enormous energies (γ x100 Kev) can be produced.

It can also been shown that Compton losses by relativistic electrons are similar to synchrotron losses, with $B^2/8\pi$ in eqs.(4.1),(4.2) replaced by the radiation energy density u_r. If, in a source, the synchrotron photons have an energy density $u_r > B^2/8\pi$

,they will be scattered to give a larger Compton energy density that exceeds the synchrotron energy density by a factor $u_r / B^2 / 8\pi$ and so on, until the photon frequency becomes so large that the Klein-Nishina regime is approached or the electrons are catastrophically cooled (the so-called Compton catastrophe).

The formalism for the non-thermal emission mechanism in an astrophysical setting has been recently reviewed by Marscher (1983). The "observable" parameters for each source are: the synchrotron turnover frequency ν_m ,the peak radio flux density F_m,the optically thin spectral index α and the angular diameter of the source θ_d . With all these observable given, one can predict the first-order self-Compton flux F_c :

$$F_c(\nu_c) = q(\alpha) \ln \Lambda (1+z)^{2(2+\alpha)} \nu_c^{-\alpha} F_m^{2(2+\alpha)} \nu_m^{-(5+3\alpha)} \theta_d^{-2(3+2\alpha)} \qquad 4.4$$

where $q(\alpha)=0.67$ for $\alpha=0.5$ and $\Lambda = \nu_b/\nu_m$,with ν_b being the high energy synchrotron cut-off. Is is worth noting what is the sensitivity of the last equation to a change in various parameters. Note a very strong dependence on the angular size of the source -for $\alpha=0.5$ $F_c \propto \theta_d^{-8}$ - and on the self-absorption frequency ν_m -for $\alpha=0.5$ $F_c \propto \nu_m^{-6.5}$ -. The dependence on the cut-off frequency is not very strong,as it only enters in a logarithmic form.

Several points should be stressed:

i) in no case a synchrotron self-absorption turnover was unambiguosly observed. Rather, the spectra in the radio band are flat,indicating a superposition of partially opaque zones;

ii)the model predicts a strong correlation between variability at X-ray and radio-IR-optical frequencies. However,there are cases where the variability time-scales are clearly different in different bands,a strong evidence for inhomogeneous models.

IV.2 BEAMING MODELS

The X-ray data reveal a gross discrepancy of several orders of magnitude between the measured flux and that predicted by the SSC theory. Several explanations were devised to reconcile that discrepancy (e.g. coherent emission processes,Compton scattering from a hot gas,etc.). Perhaps the most promising one is the scenario suggested by Rees (1966) and further developed by Blandford and Konigl (1979). In those theories,the relativistic bulk-motion or expansion of the emitting material is responsible for the diminuition (or enhancement) of the flux density. An attractive feature of such a model is its ability to confront the data in a quantitative manner with the addition of just one free parameter,the Doppler factor

$$\delta = 1/\Gamma(1-\beta\cos\phi) \qquad 4.5$$

where Γ is the bulk Lorentz factor and ϕ the velocity-observer angle. In addition, the hyphotesis that QSOs and BL Lacs contain relativistic beams unifies the otherwise disparate phenomena of superluminal motion,rapid flux variations,weak X-rays,power flow to the outer lobes,strong bending,one-sided jets, and it may also explain the statistical relationship among several classes of sources (Antonucci and Ulvestad 1985).

The most powerful argument for relativistic motion comes from the phenomenon of superluminal motion; the common model,again, involves a narrow relativistic beam, aimed nearly at us,carrying one or more luminous "blobs" or component which move away from the core. Because of the relativistic motion, the components display a large Doppler factor (blueshift) and,as with intensity variations, the timescale for transverse motion is shrunk for a stationary observer. When this is taken into account, the apparent transverse velocity is

"superluminal". If the radiation from an isotropic source is beamed toward the observer, the source appears more luminous than in its rest frame. The calculated radiation density in the source is then an overestimate of the true radiation density, and therefore the calculated Compton flux is too large. If the bulk motion has the relativistic Lorentz factor Γ, the emitted radiation, as seen in the frame of the observer, will be concentrated in a cone having an opening angle $\sin^{-1}(1/\Gamma)$, which for large Γ is $1/\Gamma$.

In practice, the argument is turned around, and the X-ray observations are used to derive a lower limit to the beaming factor δ. In fact, it is possible to write:

$$F_x(\nu) = F_c(\nu)\,\delta^{-2(2+\alpha)} \qquad 4.6$$

where F_x is the observed flux density and F_c is the value predicted for no beaming (that is to say, isotropic emission). It is instructive to see that $\delta = 1$ at the angle $\phi = \arccos[(\Gamma - 1)/\beta\Gamma]$, which for a large Γ gives $\phi \approx (2/\Gamma)^{1/2}$. Hence, for larger angles, one will see enhancement over the flux density predicted by the SSC formalism, whereas for smaller angles diminuition will occur.

It is important to note that while, as we have seen, $F_c(\nu)$ is very sensitive to θ_d, F_m as well as ν_m, δ varies as:

$$\delta \propto F_x^{-r}\, F_m\, \nu_m^{-q}\, \theta_d^{-s}\, (1+z) \qquad 4.7$$

where, for $\alpha = 0.5$, is: r=0.2, q=1.3, s=1.6. So, since r is small, the calculation is insensitive to uncertainties in the X-ray flux; ν_m is usually poorly defined, but the biggest uncertainty comes from θ_d, since it is hard to determine accurately and s is the largest of the exponents.

IV.3 INHOMOGENEOUS MODELS

The homogeneous model is clearly inadeguate in many cases. The self-absorbed (low frequency) side of the spectrum from a homogeneous synchrotron source has α =2.5 but this is rarely observed. Konigl (1980) has modelled the relativistic beam with a conical flow of high energy particles,with the particle density and magnetic field decreasing in a power-law from the apex; different frequencies are predominantly produced in different regions with possibly different Γ factors.

Ghisellini et al.(1985) investigated a class of models where the source has an elongated paraboloidal structure,going over to a conical geometry with increasing distance from the center of activity. This configuration is suggested by physical models of jets which envisage a collimated region near the core (paraboloid),due to the pressure gradient of the confining medium, where the bulk velocity of the plasma increases,followed by a region of free expansion (Begelman,Blandford and Rees 1984).

The essential difference between the two geometries is that,though the synchrotron emissivity is always a decreasing function of the radius,in the paraboloid the integrated emission from the outer zones can be larger than that of the inner zones,while this is very unlikely with a conical region. The observed spectra (e.g.BL Lacs) indicates the necessity of invoking a region with steep gradients and a conical shape,in order to explain the radio spectra (Marscher 1977), and a smaller region with slow gradients and parabolic geometry which may account for the emission from the IR to the X-ray bands,with higher frequencies originating in progressively smaller regions,which implies that the time scale of variability is expected to decrease continuosly with increasing frequency in the synchrotron spectrum. Depending on the parameters, the Compton

radiation can be predominantly produced near the origin of the paraboloid,or in the intermediate region between the paraboloidal and conical zones.

The inhomogeneous jet models are much more realistic than an homogeneous sphere but unfortunately have many parameters and cannot be simply or uniquely constrained.

IV.4 PAIR-PRODUCTION EFFECTS

Powerful X-ray emission is,as we have seen,a common feature of active galaxies, some of which -i.e. 3C 273,NGC 4151,CEN A,MCG 8-11-11,NGC 1275- have also been detected as gamma-ray sources. The observed high luminosities, coupled with reports of variability on time scales of days or less at X-ray energies -and in the hyphotesis that X ang gamma ray emission originate in the same volume-,imply that electron-positron pair production can take place as a result of X-ray photons collisions with gamma-ray photons (Herterich 1974):

$$\gamma + \gamma \longrightarrow e^- + e^+$$

The absorption of a gamma-ray of energy E_γ by pair production with an X-ray photon of energy E_x,has a threshold at:

$$E_T = 2m_e c^2 / (E_\gamma (1-\cos\theta))$$

where θ is the angle between the momentum vectors of the two photons. For fixed values of E_γ,the cross section $\sigma(E_x)$ for the process rises rapidly from a threshold of $E=E_T$ to a maximum value of 1.7×10^{-25} cm^{-2} at $E=2E_T$ and falls off as E^{-2} for photon energies $E>>E_T$.

The optical depth for this process can be written as :

$$\tau_{\gamma\gamma}(E_\gamma) = R \int \sigma(E_x) N_x(E_x) dE_x$$

where the cross-section σ and the density of X-ray photons per unit energy N_x are assumed to be constant throughout the source region of size R. Following Herterich(1974), for simplicity we set $\theta = \pi/2$;furthermore,within the limits of accuracy required by this calculation it is sufficient to approximate $\sigma(E_x)$ by a rectangular function of height σ_{max} and width $2.5E_T$. Consequently,the optical depth may be written as:

$$\tau_{\gamma\gamma} = R\,\sigma_{max}\,N_x(2E_T)\,2.5\,E_T \quad .$$

To estimate N_x we use the X-ray luminosity and write:

$$N_x(2E_T) = f(\alpha)\,L_x\cdot(2E_T)^{-(\alpha-1)}/4\pi R^2 c$$

where α is the source spectral index at X-ray energies. For L_x taken over a fixed energy band (generally 2-10 Kev), $f(\alpha)$ is a slowly varying function of α. Introduction of numerical values leads to the final expression:

$$\tau_{\gamma\gamma} = 2.5\times10^{-28} f(\alpha)\,L_x/R\,(2E_T)^{-\alpha} \qquad 4.8$$

with L_x in erg/s,R in cm ,E_T in Kev,and α =0.6 . The crucial quantity L_x/R is often referred as the "compactness parameter".Thus in compact and very luminous source, pair creation may play a key role. In addition to suppressing gamma-ray emission from the source, pair creation modifies the spectrum at all lower frequencies,because the energy which would otherwise be emitted in the gamma-spectrum has (because of pair production) to be channelled into other wavebands.

Table 2 lists the values of L_x and $R=c\,\Delta t$,together with the optical depth $\tau_{\gamma\gamma}$ at different gamma-ray energies, for the observed gamma-ray sources.Note,in particular, the high optical depth that characterizes the object 3C 273; the conseguence of this will be

discussed in chapter V.

The very rapid timescales of variability detected in Blazars imply that they must either be beamed or have spectra which fall off steeply at hard X-ray energies. Otherwise, a "false photosphere" of e^--e^+ pairs would scatter the optical continuum,destroying its high polarization and smearing out the rapid variations (Rees 1985).

TABLE 2

NAME	CLASS	R	L_x	1Mev	10Mev	100Mev	500Mev
3C 273	QSO	1.1×10^{15}	1.1×10^{46}	13.5	54	214	563
NGC 4151	Sey 1	2.0×10^{13}	6.2×10^{42}	0.4	1.7	6.64	17.4
NGC 1275	BL Lac	2.5×10^{15}	6.3×10^{43}	0.03	0.13	0.54	1.44
CEN A	RG	2.2×10^{14}	1.8×10^{42}	0.01	0.04	0.18	0.5
MC 48-11-11	Sey 1	5.0×10^{15}	8.3×10^{43}	0.002	0.008	0.003	0.12

CHAPTER V 3C 273 AND "BLAZARS"

V.1 3C 273:RADIO-MORPHOLOGY

The quasar 3C 273 is very bright both optically ($z=0.158, m_v=1.3$) and in the radio range (~30 Jy at 50 Ghz),so that a large amount of observational data has been accumulated over the years. An optical jet extends from a distance of ~10 arcsec to 25 arsec from the quasar (with $H=100h, q=0.5$, $1"=1.84/h$ pc).The projected length of the jet is 42/h Kpc. The radio emission comes principally from two locations: a compact flat-spectrum component centered on the nucleus of the quasar, and a more diffuse component coincident with the optical jet.

The compact radio source has been a principal object of study by VLBI and studies of its compact structure soon indicated internal superluminal motions, with apparent speed $v/c=5.5/h$,of compact components or "knots",relative to the stationary core. No counterjet emission has been found, and this absence could result from beaming; even a relatively modest jet speed yields a large jet/counterjet flux ratio. Fig.9 shows three maps of the compact radio structure at 10.7 Ghz (Unwin et al. 1985). These maps show that the basic structure always consists of a bright core -labeled D- at the eastern end and one or more knots -labeled C_i- extending out to 20 mas. The results of measuring the radial distances of the various components from the core are plotted on the time sequence shown in fig.10. Both C_3 and C_4 are superluminal relative to the core D (see table 3), with no evidence of acceleration. Fig.11 plots the peak brightness of the core D and and the knot C_3 as a function of the observing epoch; also shown is the variation in the total flux density. Component C_3 shows an exponential decay with

half-life ~ 2.5 yr at 10.7 Ghz. Component D is probably stationary; in the relativistic jet hypothesis, its decay could result from a reduction in the flux of relativistic fluid.

In this picture of components being ejected from the core and decaying as they move out, the total flux density varies much less than the individual knots, since no single component dominates at any time. VLBI observations show non-linear structure, and this is evident in fig.12, where the positions of all the components are plotted, with a total bending of at least 21°. The jet is then straight for a range ~ 1000 in radius. Curvature is seen in other compact sources, suggesting bending of jet by pressure gradients and amplification by geometrical effects. VLBI maps also make it possible to determine the spectra of individual components, and these spectra are shown in fig.13. There are several points to note;

i) individual components have spectra different from one to another and from the total flux density, whose spectrum is flat and smooth;

ii) the jet components C_3 and C_4 have straight spectra with $\alpha = 1$ and $\alpha = 0.7$ respectively, indicative of optically thin synchrotron radiation. Because no lower frequency VLBI observations separate the components reliably, only upper limits to their synchrotron turnover frequencies can be deduced;

iii) the core D is optically thick below ~ 70 Ghz with $\alpha = -0.65$ and clearly it cannot be approximate at all well by a homogeneous self-absorbed synchrotron source for which $\alpha = 2.5$. More likely it is a blend of components with a range of turnover frequencies.

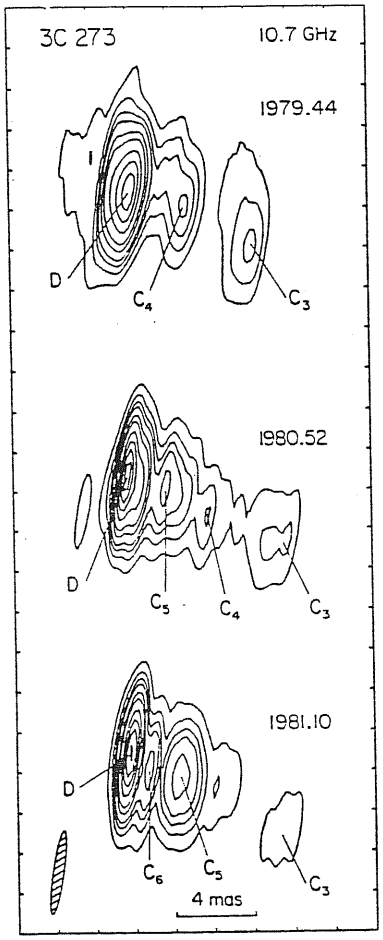

Fig. 9

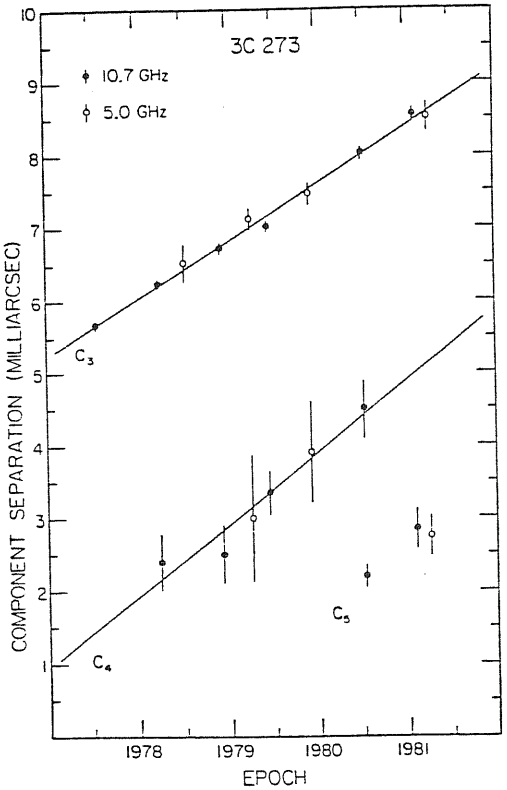

Fig. 10

Fig.9: Radio maps of the compact radio structure in 3C 273 at 10.7 Ghz (from Unwin et al.1985).

Fig.10: Separation of components in 3C 273 jet from the core at 5.0 and 10.7 Ghz.

TABLE 3

Superluminal motion in the 3C 273 jet

Component	C_3	C_4
Proper motion (mas/yr).....	0.79	0.99
Apparent transverse velocity*.....	5.5/h c	.7/h c
Epoch of zero separation (yr)	1970	1976

* Relative to the core D (H_o=100h Km/sec/Mpc).

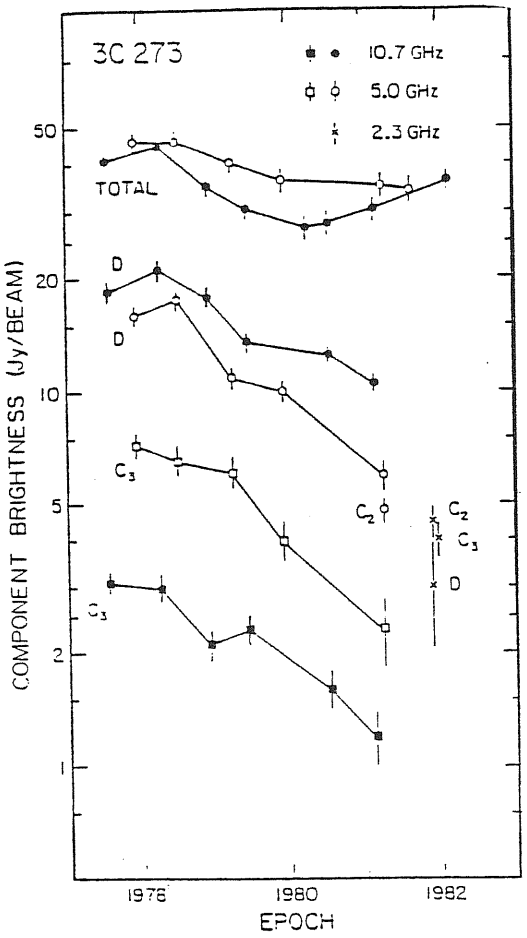

Fig. 11

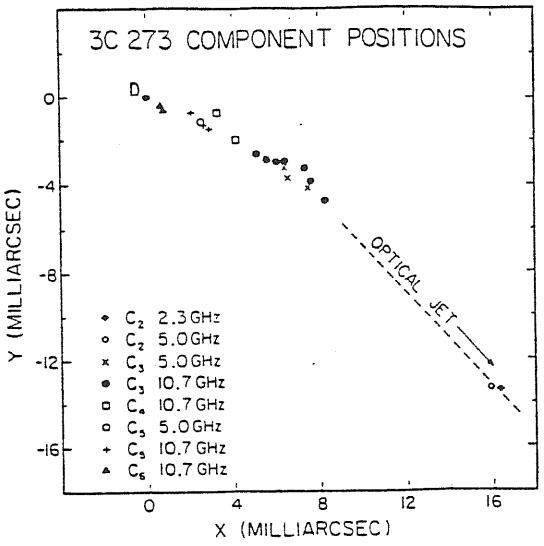

Fig. 12

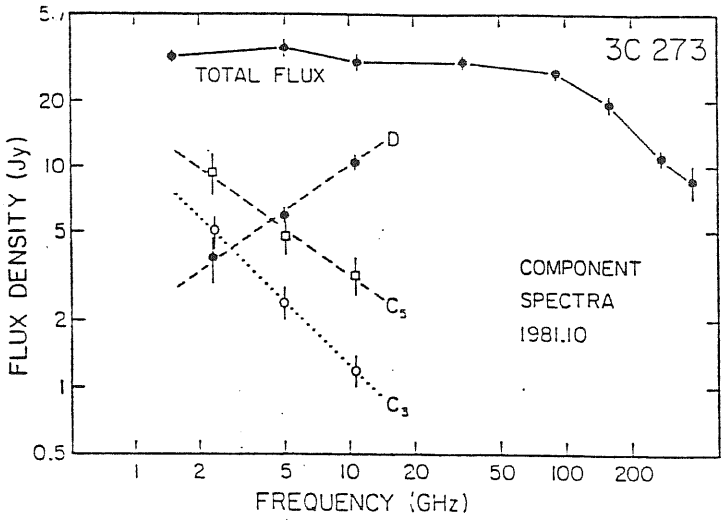

Fig. 13

Fig. 11: Variation in peak brightness of component D and C_3, at 5.0 and 10.7 Ghz as a function of observing epoch. The variation in total flux density is also shown (Unwin et al.1985).

Fig. 12: Positions on the sky of knots in the jet of 3C 273, relative to the compact core.

Fig. 13: Radio spectra of the core D, and knots C_3 and C_5. Also shown is the total flux-density spectrum (from Unwin et al.1985).

V.2 3C 273: THE OVERALL SPECTRUM

The source 3C 273 has the best studied spectrum of all quasars, since it has been observed in every accessible wave-band from 22 Mhz to 800 Mev. In the radio-range, as shown, the spectrum is smooth and flat; above 70 Ghz it steepens to $\alpha = 0.7$ (Clegg et al. 1983) and steepens again to $\alpha = 1$ in the near IR ($\sim 10^{14}$ cm). 3C 273 shows the optical-UV excess over the IR power-law referred to as the "3000 A bump" that is prominent in many quasars and Sey 1s spectra. Malkan and Sargent (1982) spectrum decomposition is showed in fig.15; the dominant component in the UV is blackbody emission with best-fit temperature $T_{BB} \simeq 26{,}000$°K and surface emitting area of 3×10^{33} cm. As already discussed in III.3, the most likely interpretation of the thermal bump is that it comes from an accretion disk. This optical component is also less variable and less polarized than the radio, strengthening the conclusion that it probably arises from a different region than the radio-IR radiation.

The X-ray emission lies roughly on the $\alpha \simeq 1$ extrapolation from the IR but it has a flatter spectral index ($\alpha = 0.44$ in the 1-10 Kev range, $\alpha = 0.7$ in the 13-120 kev) (Halpern 1982).

3C 273 is, up to now, the only quasar identified as an high energy gamma-source ($\alpha_\gamma \simeq 1.5$). Extrapolating the hard X-ray and COS-B gamma ray data points up to 5 Mev, the total X-gamma ray luminosity output would be $\sim 2.25 \times 10^{47} h^{-2}$ erg/s (Bassani, Dean and Sembay 1983). The source is variable at most frequencies and over a wide range of timescales, with shorter timescales at higher frequencies (see table 4). A bolometric luminosity of $L_B \simeq 2 \times 10^{47}$ erg/s implies, in the accretion picture, a BH of mass $M > 1.5 \times 10^9 M_\odot$ (for $L = L_E$) and a corresponding gravitational radius $r_G = 5 \times 10^{14}$ cm, very close to the X-ray time variability indications ($R = 1.1 \times 10^{15}$ cm).

TABLE 4
Luminosities and variability timescales in different energy bands

L_{radio} (1-22)x 10^9 Hz	6.8×10^{44}	years
L_{opt} (5-7)x 10^{14} Hz	5.7×10^{45}	months
L_x (2-10) Kev	1.2×10^{46}	1/2 day
L_{gamma} (50-500) Mev	3.2×10^{47}	?

$h = H_o/100 = 1/2$

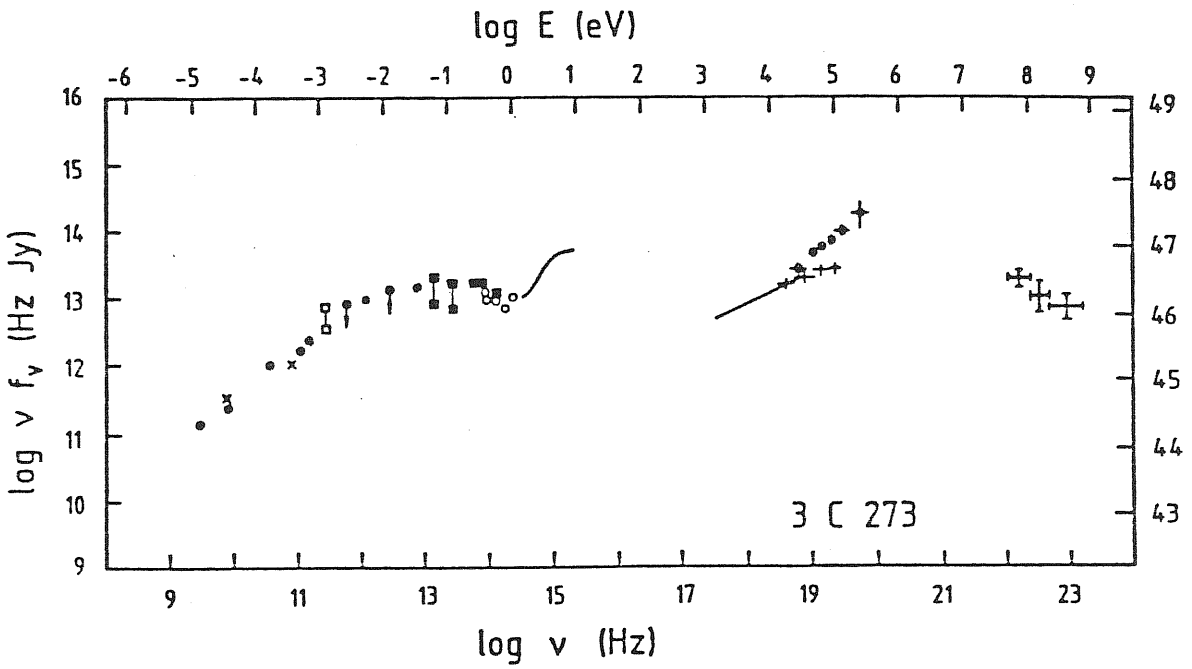

Fig. 14

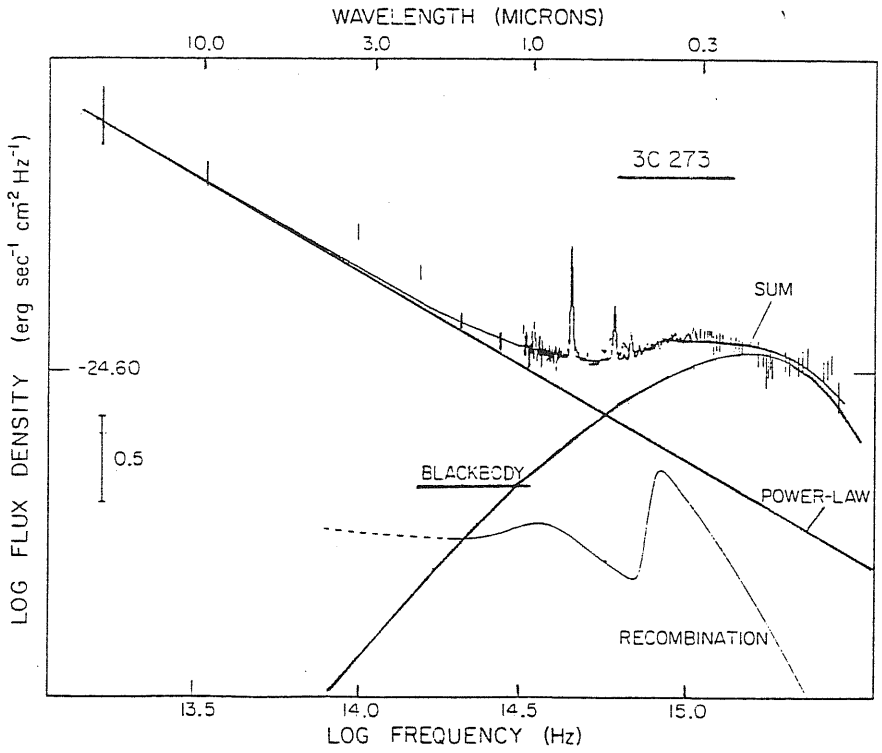

Fig. 15

Fig. 14: Overall energy spectrum of 3C 273.

Fig. 15: Decomposition of the 3,000 A bump in 3C 273. Three solid lines illustrate the power-law, hydrogen recombination and blackbody component at T= 26,000 K (from Malkan & Sargent 1982).

V.3 3C 273: INTERPRETATION

V.3a: The Knot

As a model of VLBI structure we assume that the jet component C_3 is a homogeneous sphere containing a tangled magnetic field B and ultrarelativistic electrons which are isotropic in the comoving frame. The electrons produce radio emission by synchrotron radiation and the X-ray flux (at least in part) by inverse-Compton scattering off their own synchrotron photons. A constraint on these models is that the IC X-ray radiation should not exceed the observed X-ray flux. For the sphere model, this gives a lower limit to the beaming factor .

We calculated the self-Compton X-ray radiation using formulae given by Marscher (1983) -see IV.2-. This calculation yields both the intensity of the X-rays and their spectral index, which is the same of the optically thin radio index (cf IV.2). The observational parameters we use for the knot C_3 are listed in table 5; we derived $\delta\,(C_3)>1$. Unfortunately, as already noted, the factor δ is very sensitive to the assumed self-absorption frequency. A small change in the assumed ν_m -e.g. $\nu_m=1, F_m=12$- would boost the δ factor up to $\delta>5$.

An alternative way we have to determine the beaming factor is , of course, by superluminal motion. The minimum Lorentz factor Γ_{min} associated with the observed superluminal velocity is $\Gamma_{min}=\delta_{SL}=\beta_{obs}=5.5/h$ which, in turn, implies a viewing angle of 10° h (see fig.16).

Probably the most straightforward way we have in these case to derive δ is by variability arguments. We know that the half-life of component C_3 at 10.7 Ghz is $\tau=2.5$ yr and, at the same frequency, the measured angular dimension of C_3 is 2.1 mas, substantially bigger than $c\tau/(1+z)$, the light travel distance

for the observed variability timescale. The best explanation for this is, again, relativistic motion with $\delta_t \gtrsim 3/h$,quite close to the value of δ_{SL} . It must be stressed that,while SSC conclusions are independent on H_o (if the angular size is measured with VLBI), superluminal motion and variability timescales depend on the actual value of H_o. It is also worth emphasizing that the radio spectral index of knot C_3 is much steeper than that of the X-rays, so it seems unlikely that tha X-rays are due to IC scattering in C_3; in these respects we have been conservative in the sense of minimizing the allowed value of δ .

A viewing angle $\phi \simeq 10^\circ$ h has an obvious consequence for the appearance of the curved jet (see V.1); any component of the bend perpendicular to the plane P_o containing the initial jet direction and the line of sight will be amplified by a factor $\sim 1/\sin\phi$, thus implying the intrinsic bend to be:

$$\Delta\theta \approx 3.6^\circ h$$

and partially solving the strong curvature problem. The component $\Delta\theta$ of the jet curvature in the plane P_o is less constrained.

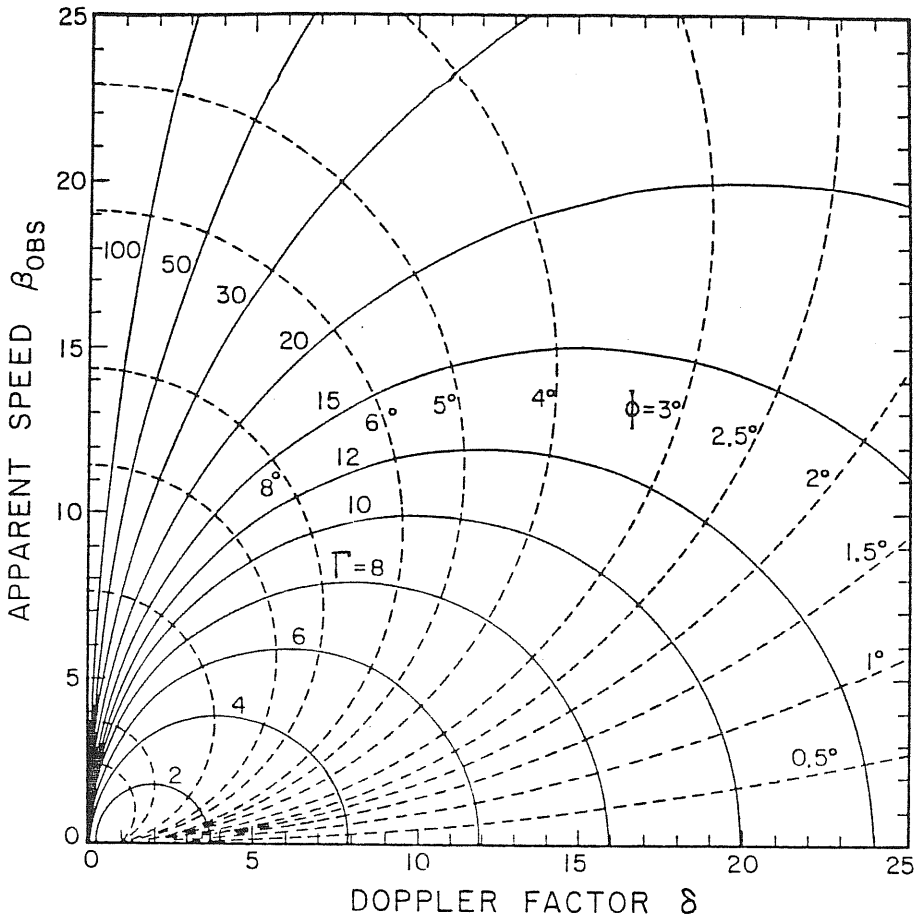

Fig. 16

Fig.16: Kinematic properties of a relativistic beam. Curves of constant Lorentz factor Γ (solid lines), and constant angle ϕ of the beam to the line of sight (dashed lines), are shown as functions of the observable quantities δ, the doppler factor, and β_{obs}, the apparent transverse velocity. The Lorentz factor takes the value Γ =1 at the point β_{obs} =0, δ =1.

TABLE 5
FACTOR DETERMINATION FOR COMPONENT C_3

PARAMETERS	
ν_m(Ghz)	$\leqslant$ 2
F_m(Jy)	$\geqslant$ 6
θ_d(mas)	2.1
Δt(yr)	2.5
α	1
F_x(Jy at 1Kev)	3.2×10^{-5}
δ	1.
δ_{SL}	5.5/h
δ_τ	3/h
ϕ	10°

V.3b:The core

The core D represents the region surrounding the "central engine", which powers both the VLBI jet and the optical jet. However,it is obvious from the optically thick slope of $\alpha = 0.65$ that a homogeneous synchrotron model is inadeguate and that a more elaborate model, as an inhomogeneous jet-model, is required. Neverthless,for the sake of clarity,we shall consider here a multicomponent model.

The size of the core is 0.8 mas at 10.7 Ghz where,as shown in fig.13, the core is still optically thick. An indication of the existence of different components in the core comes from time variability. For example, the X-ray flux half-day variability timescale implies,through the causal argument, an angular size $\theta_x \leq 4 \times 10^{-4}$ which could be reconciled with the core size of 0.8 mas only with an unphysically high Doppler factor $\delta \geq 2000$.

The existence of a mm-IR component was recently pointed out by Robson et al.(1983). Fig.17 shows the mm-IR spectrum flaring up with a timescale $\tau \approx 1$ month and sharply peaked at 300 Ghz which is indicative of synchrotron self-absorption; the optically thin spectrum can be fitted by a power-law of spectral index $\alpha \approx 1$. Again, the IC X-ray radiation from this component should not exceed the observed X-ray flux. The lower limit to the beaming factor thus derived is $\delta_{IR} > 4$ (with $h=0.5$; $\delta_{IR} > 2.6$ with $h=1$), indicating the presence of relativistic bulk motion in the inner zone where the IR emission is coming from; the intrinsic size of the IR emission region is $R_{IR} = 2.6 \times 10^{16}\ \delta$ cm $\approx 1 \times 10^{17}$ cm.

Now the apparent dimension of the X-ray component is $R_x \approx 1.1 \times 10^{15}$ cm. In the absence of relativistic beaming, the compactness parameter L_x/R_x is such that the gamma-rays should be absorbed by photon-photon pair production processes (see IV.4). Thus, the high 3C 273 gamma-ray output has been usually interpreted

as coming from a much larger size of 1pc (e.g. Bassani and Dean 1981). In fact, the pair production optical depth for 3C 273 can be written as :

$$\tau_{\gamma\gamma}(\nu) \simeq 9 \cdot \left(\nu/10^{20}\right)^{\alpha} / R_{15}$$

(cf eq. 4.8). At the break energy (where $\tau_{\gamma\gamma} \simeq 1$), photon absorption causes the intensity to break from $I_\nu \propto \nu^{-\alpha}$ to $I_\nu \propto \nu^{-\alpha}/\tau_{\gamma\gamma}(\nu) \propto \nu^{-2\alpha}$; the optically thick emission above the break frequency actually emerges from an increasingly narrower surface layer as $\tau_{\gamma\gamma}$ increases (Svensson 1985). This very simple picture seems to fit fairly well the observed steepening in 3C 273 from hard X-rays ($\alpha \simeq 0.7$) to gamma-rays ($\alpha \simeq 1.5$) with an extrapolated break frequency close to 1Mev (fig.18). However, the reprocessing of radiation by $e^+ - e^-$ pairs has not been taken into account; the effect of the feedback will tend to steepen the X-ray power-law spectrum towards $\alpha = 1$ (e.g. Kazanas 1984).

Relativistic beaming can completely alter the picture; $\tau_{\gamma\gamma}$ actually scales with δ^{-4}. A Doppler factor $\delta = \delta_{IR} \gtrsim 4$ would be enough to make the source optically thin up to 500 Mev, but this would have dramatic effect on the intrinsic spectrum. In particular, the power of the thermal bump (which is isotropic) relative to the intrinsic power-law continuum should be quite unusual (fig.19). The luminosity in bulk motion would be a small fraction of the total radiative output, especially in the case of an electron-positron beam. The results for both the mm-IR and X-ray component are summarized in table 6. It is also worth emphasizing that, for a viewing angle $\phi \simeq 10^\circ$, $\delta = 4$ corresponds to $\Gamma = 2.4$, a mildly relativistic Lorentz factor that could perhaps be ottained by radiative acceleration in the funnel of a thick accretion disk. However, at such viewing angle, we would expect to see the very

inner funnel ($T \gtrsim 10^5$ °K) thermal component ,which is not seen.

TABLE 6

	R(size)	δ	L_{bulk}(erg/s)
Component IR	1.0×10^{17}	4	$1.7 \times 10^{45}\ m_p/m_e/\gamma_{min}^{2\alpha}$
Component X	4.4×10^{15}	4	$1.7 \times 10^{44}\ m_p/m_e/\gamma_{min}^{2\alpha}$

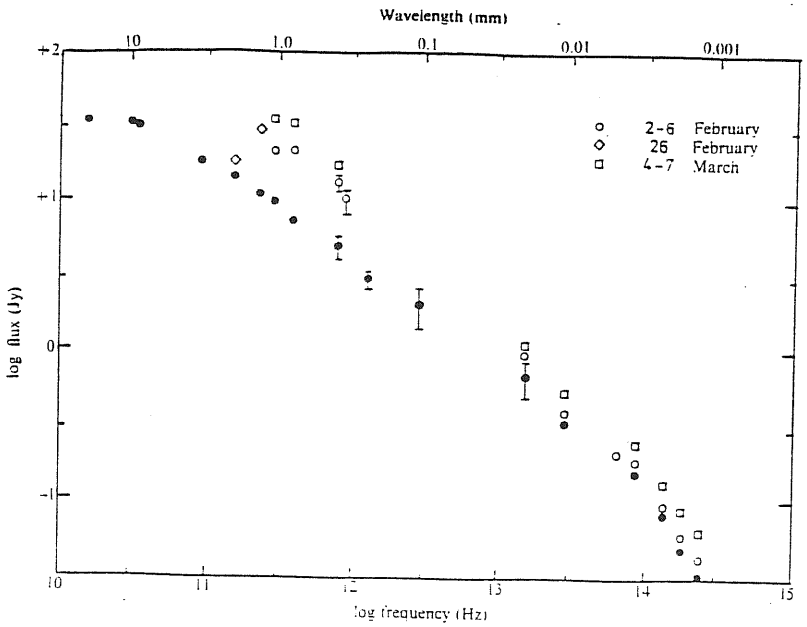

Fig.17

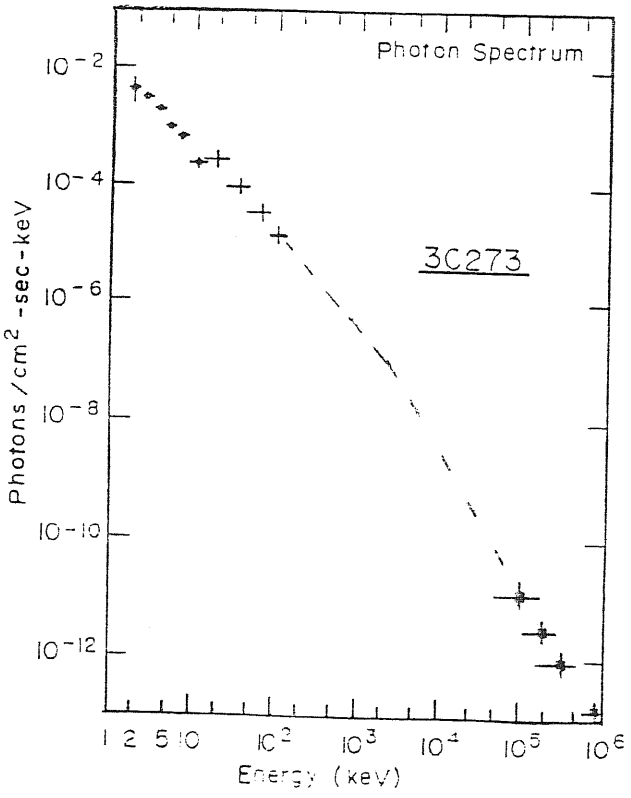

Fig. 18

Fig.17: mm-IR flare of 3C 273 (Robson et.al. 1983)

Fig.18: Observed hard X-ray (α =0.7) and gamma-ray spectrum of 3C 273.

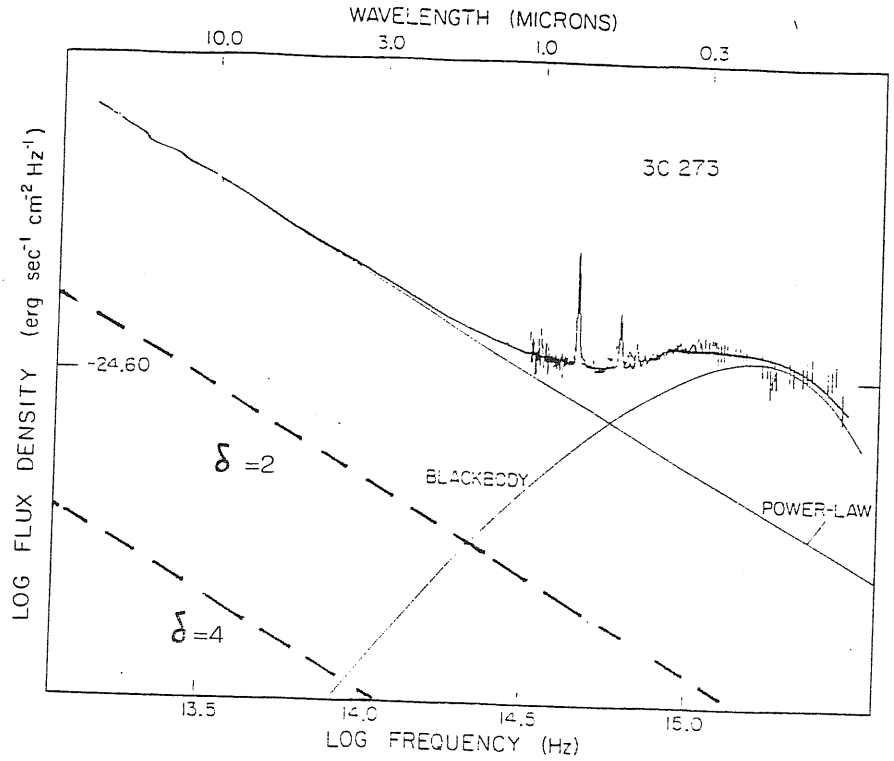

Fig.19

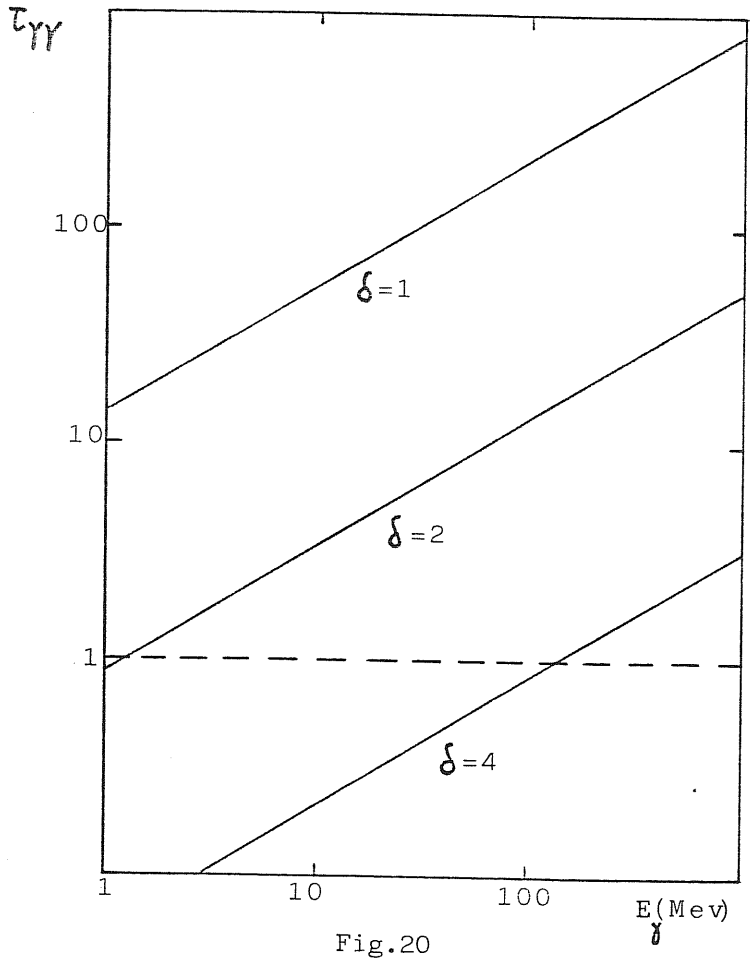

Fig.20

Fig.19: Intrinsic power-law continuum (dashed-lines) for two values of the beaming factor δ .

Fig.20: Photon-photon optical depth at different energies for different values of the beaming factor δ.

V.4 THE BLAZARS

There are very few objects in the literature with such detailed observations as those shown for 3C 273. A different approach must be followed, e.g. an investigation of the beaming hyphotesis for a class of objects such as the Blazars. This word denotes the union of two categories of active galactic objects, the BL Lacs and the OVV quasars. The OVVs are intrinsically different from BL Lacs since they have luminous broad lines, but they have all of the special features of BL Lacs. The constraints placed by the rapid variability and high polarization are so severe that a stationary, unbeamed synchrotron model of the emission region is difficult to construct; superluminal motions, as well, indicate that directed relativistic motion is fairly common among Blazars.

We have considered the applicability of SSC formalism to a sample of $\approx$ 40 Blazar objects for which radio VLBI sizes and flux densities are available in addition to the X-ray data; again, we have used this formalism to predict the X-ray flux density at 1 Kev as inferred from the radio data and compare it to the observed values, in order to determine the Doppler factor δ . Previous attempts in this direction were made by Madejski and Schwartz (1983) on a sample of 16 BL Lacs (note that there is an error in their formula for the Compton flux; therefore the derived δ is underestimated by a factor 2) .It is important to stress that we have used only the angular source diameters measured by VLBI techniques. Previous estimate of δ based on X-ray fluxes have been derived from the X-ray variability (Urry and Mushotzky 1982) or electron lifetime arguments (Worral et al. 1982), and give values in the range 20-165; this can be misleading since, due to inhomogeneity in the source, the regions of variable X-ray emission may not be coincident with the radio emission regions which are of interest here.

The parameters needed to determine the Doppler factor δ are (eq.4.5,4.6): the synchrotron turnover frequency ν_m (in Ghz); the radio flux density F_m(in Jy) at ν_m ;the source angular diameter θ_d (in mas); the redshift z; the upper cut-off frequency ν_b (in Ghz); the spectral index α of the optically thin radio component, $F_\nu \propto \nu^{-\alpha}$;and the observed X-ray flux at 1 Kev.

It is important to emphasize that the sample of objects we have used is not complete in any statistical sense,since no uniform definition or survey for Blazars exists. Neverthless, this is a substantial and quasi-random subset of all the objects commonly considered in this class. We shall keep this limitation in mind in drawing the conclusions below.

Table 7 lists the objects under study. The first column gives the coordinate names, with other commonly used names in column (2). The diameters of the sources are listed in column (3); the frequencies of the VLBI measurements and the corresponding flux densities are given in column (4) and (5). The redshift are given in column (6),where available. For the objects with no redshift information, we have adopted z=0.4, corresponding to the average redshift for all Blazars (note that $\delta \propto (1+z)$). We have considered the observed steepening of the Blazar spectra between IR and optical frequencies ($\approx 10^{14}$ Hz) as an indication of the synchrotron high energy cut-off, and consequently adopted $\nu_b = 10^5$ Ghz; note that our prediction is rather insensitive to that value ($\delta \propto (\ln \Lambda)^{0.2}$;see IV.2).

The synchrotron turnover frequency ν_m is not measured in general. For our prediction to be unique, we must also assume that only one component contributes to the X-ray flux. The highest reasonable value of ν_m for this component must be the frequency of the VLBI measurements. We have also assumed a uniform spectral index α =0.75 for the optically thin component, as indicated by Landau et

al.(1983). The measured X-ray fluxes are given in column (7). Column (9) gives the beaming factors δ inferred from the model.

Strictly speaking, our calculation places only a lower limit to the predicted X-ray emission. The conflict can be resolved, ad hoc, for the sources where the measured X-ray flux density exceed the prediction ($\delta < 1$) by assuming an additional component of SSC X-ray emission. In addition, there possibly could exist another mechanism generating X-ray in those objects. The distributions of δ are plotted as the histograms in fig.21. OVV quasar seem more beamed, as a class, than BL Lacs, but more objects need to be included. The shaded areas correspond to superluminal sources; these are characterized by high Doppler factors, as it should be.

We have been looking for stronger consistency checks. The basic hyphotesis of this work is that the radio core emission is anisotropic;we also know that the off-nuclear radio emission is likely to be isotropic,since it is usually two-sided (no Doppler favouritism effect),in the form of a halo, or at least diffuse. The ratio of the core to extended radio emission has been studied as a possible indicator of viewing aspect or beaming intensity. It is found to correlate with optical polarization, optical and radio variability, and one-sided radio morphology (Antonucci and Ulvestad 1985). This ratio is given in column (8), whereis known. We have found a strong correlation between this ratio and our δ-distribution; we still don't know if this correlation is a real or an induced one. If real, this result would confirm the validity of the relativistic beaming hyphotesis.

TABLE 7

Doppler-factor distribution for Blazars

BL Lacs

NAME		θ_d	ν_m	F_m	z	F_x(1Kev)	S_c/S_{ext}	delta
0048-097	OB 081	0.4	5	0.71	.....	6.6 (-8)	8.1	1.92
C133+476	C 457	0.7	5	1.37	0.86	9. (-8)		1.98
0212+ 73		1.2	5	1.5	.....	2.27(-7)		0.54
0219+428	3C 66A	1.5	5	0.2	0.444	1.6 (-7)	0.6	0.06
0235+164	AO	0.5	5	1.75	0.852	1.7 (-7)	59.7	4.3
0306+102	PKS	0.5	5	0.73	.....	2.02(-7)		1.12
0316+ 41	NGC1275	3.0	5	38.3	0.0172	2. (-5)	31.41	1.15
0454+ 84		1.1	5	1.3	.....	5.2 (-8)		0.7
0521-365	PKS	1.5	5	0.86	0.0554	1. (-6)	0.3	0.14
0716+ 71		0.7	5	0.5	.....	2.2 (-7)		0.44
0735+178	OI 158	0.3	5	0.8	0.424	3.4 (-7)	808	3.06
0754+100	OI 090	0.6	5	0.53	.....	1.7 (-7)	12.1	0.62
0818-128	OJ 131	0.8	5	0.47	.....	7. (-8)	1.5	0.4
0829+046	OJ 049	0.9	5	0.26	.....	1.9 (-7)	8	0.15
0851+202	OJ 287	0.3	5	2.9	0.306	1.2 (-6)	995	8.08
1101+384	MKN421	0.9	5	0.32	0.031	1. (-5)	2.8	0.08
1147+245	B2	0.9	5	0.39	.....	8. (-8)	22.7	0.27
1215+303	ON 325	0.7	5	0.33	.....	1. (-6)	1.6	0.22
1219+285	ON 231	1.1	5	0.72	0.102	4.2 (-7)	866	0.24
1400+162	MC3	1.4	5	0.08	0.244	1. (-7)	0.4	0.03
1538+149	4C14.60	0.8	5	0.7	.....	1.5 (-7)	7.8	0.53
1652+398	MKN501	1.	5	0.39	0.0337	1.1 (-5)	19.9	0.08
1749+096	4C09.57	0.2	5	1.43	.....	3.5 (-7)	585	8.9
1803+ 78		0.8	5	1.8	.....	1.5 (-7)		1.35
1807+698	3C 371	1.4	5	1.21	0.05	6. (-7)	1.3	0.25
2200+420	BL Lac	0.4	5	1.6	0.069	1.06(-6)	78.4	2.33
2201+044	PKS	0.7	5	0.16	0.028	3.2 (-7)	3.67	0.11
2207+ 77		0.8	5	1.17	.....	1. (-7)		0.95
2254+074	OY 091	1.	5	0.14	.....	9.7 (-8)	13.5	0.08

OVVs

0923+392	4C39.35	0.6	5	3.2	0.698	4. (-7)		4.6
1253-055	3C 279	0.4	5	1.6	0.538	1.4 (-6)	1.9	3.2
1308+326	B2	0.5	5	1.97	0.996	3. (-7)	17.3	3.8
1641+399	3C 345	0.3	10.7	6.9	0.595	1. (-6)	5.9	7.25
2223-052	3C 446	0.4	10.7	2.2	1.404	9.2 (-7)	0.14	2.19
2230+114	CTA102	0.5	5	3.5	1.037	3.4 (-7)	7.8	6.17
2251+158	3C454.3	0.3	5	0.9	0.859	5.6 (-7)		4.1

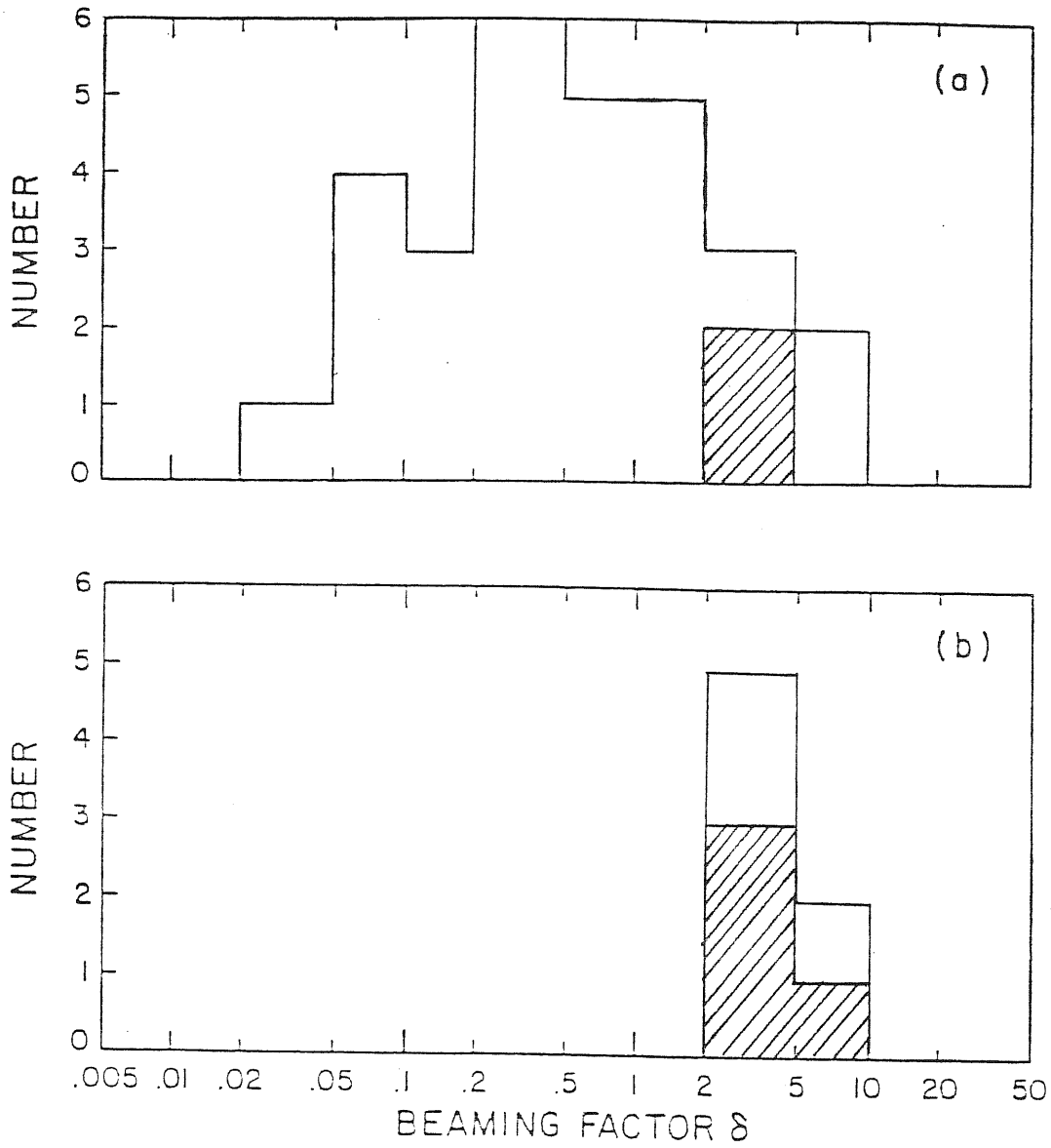

Fig.21

Fig.21: Histograms of the beaming factors listed in table 7.
Distribution for:
a) BL Lac objects;
b) OVV quasars.
Shaded areas correspond to superluminal sources.

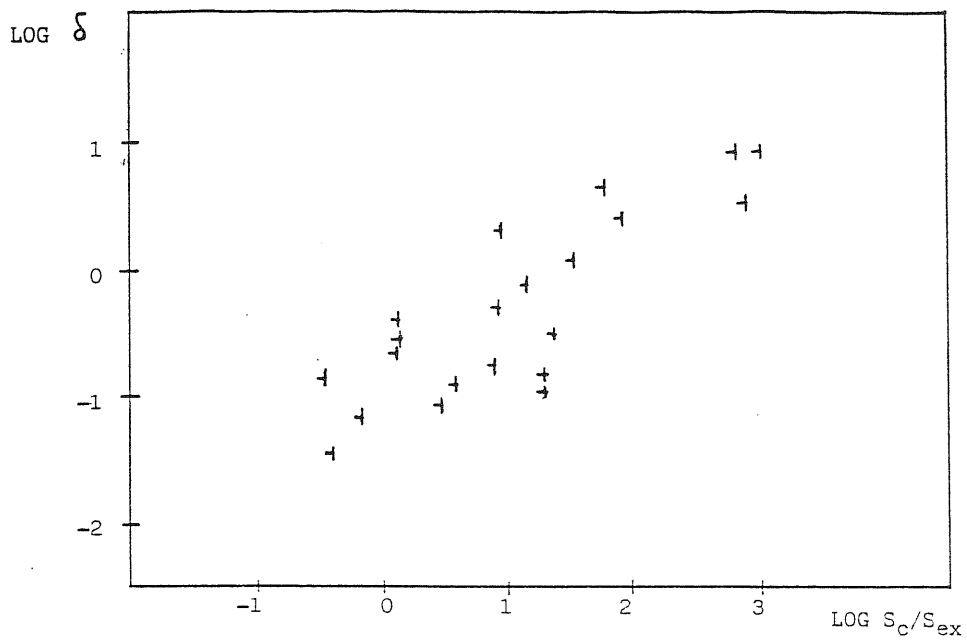

Fig.22

Fig.22: Correlation between δ and $S_{core}/S_{extended}$; number of objects=21; linear correlation coefficient r=0.81; uncorrelated parent population probability $P \ll 10^{-3}$.

REFERENCES FOR BLAZARS DATA

- Angel & Stockman ,1980
- Antonucci & Ulvestad 1985
- Bierman et al.,1981
- Eckart et al.,1982
- Landau et al.,1983
- Ledden & O'Dell,1985
- Madejski & Schwartz,1983
- Marscher et al.,1979
- Moore & Stockman,1984
- Pauliny-Toth et al.,1981
- Pearson & Readhead,1981
- Weiler & Johnston,1980
- Zensus et al.,1984

CONCLUSIONS

In this thesis we have tried to suggest what might be a fruitful approach to the study of Active Galactic Nuclei. In particular, synchrotron self-Compton models can give constraints on the physical conditions in the emission region and provide evidence for relativistic bulk-motion; the 3C 273 gamma-ray problem and the Doppler factor distribution for Blazars can be considered as investigations on this line.

Observations can also favour one or another of the proposed accretion flow patterns; the 3000 Å thermal emission feature, in particular, could support a thick accretion disk model.

Both these approaches (i.e. non-thermal models and thick disk models) are worth investigating in the attempt to reach a better understanding of Active Galactic Nuclei.

Acknowledgments:
I would like to thank Marek Abramowicz for his encouragement and scientific guidance, and Gabriele Ghisellini for a very helpful collaboration.

REFERENCES

- Abramowicz,Calvani & Nobili 1980,Ap.J. 242:772
- Abramowicz,Jaroszynski & Sikora 1978,Astron.Astrophys. 63:221
- Abramowicz & Nobili 1982,Nature 300:506
- Angel 1969,Ap.J.158:119
- Angel & Stockman 1980,Ann. Rev. of A.&A. 18:321
- Antonucci 1983,Nature 303:158
- Antonucci & Ulvestad 1985,Ap.J. 294:158
- Balick & Heckman 1982,Ann. Rev. of A.&A. 20,431
- Bassani & Dean 1981,Nature 294:332
- Bassani,Dean & Sembay 1983,Astron.& Astrophy. 125:52
- Begelman 1984,Proceedings of the 1984 Santa Cruz Summer Workshop,J.S.Miller ed.
- Begelman,Blandford & Rees 1984,Rev. Mod. Phys. 56 :255
- Bierman et al. 1981,Ap.J. 247:L53
- Blandford 1984,in Proceedings of the Manchester Conference on AGNs,ed.J.Dyson,in press
- Blandford & Konigl 1979,Ap.J. 232:34
- Blandford & Rees 1974,MNRAS 169:395
- Blumenthal & Gould 1970,Rev.Mod. Phys. 42:237
- Carrasco,Dultain-Hacyan & Cruz-Gonzales 1985,Nature 314:146
- Clegg et al.1983,Ap.J. 273:58
- Crawford et al. 1985,Nature 315:467
- Eckart et al. 1982,Astron.& Astrophys.108:157
- Elliot & Shapiro 1974,Ap. J.192:L3
- Fabian 1979,Proc. Roy. Soc. Lond.A,366:449
- Fabian & Rees 1979,in X-ray Astronomy,eds. Baity & Peterson,Oxford Pergamon
- Gaskell 1985,Nature 315:386
- Ghisellini,Maraschi & Treves 1985,Astron.& Astrophys.146:204
- Guilbert,Fabian & McCray 1983,Ap.J. 266:466
- Halpern 1982,Ph.D. thesis,Harvard University
- Hazard 1979,in Active Galactic Nuclei, Hazard & Mitton eds.(Cambridge Un. Press)
- Herterich 1974,Nature 250:311
- Hills 1975,Nature 254:295
- Hutching & Campbell 1983,Nature 303:584
- Jones,O'Dell & Stein 1974,Ap.J.188:353
- Kazanas 1984,Ap.J. 287:112
- Konigl 1981,Ap.J. 243:700
- Landau et al.1983,Ap.J. 268:68
- Lawrence & Elvis 1985,preprint
- Ledden & O'Dell 1985,preprint
- Lightman 1982,Space Sci. Rev. 33:335
- Lo et al. 1985,Nature 315:124
- Madejski & Schwartz 1983,Ap.J. 275:467
- Malkan 1983,Ap.J. 268:582
- Malkan & Sargent 1982,Ap.J. 254:22
- Maraschi et al.1985,preprint
- Marscher 1977,Ap.J. 216:244
- Marscher 1983,Ap.J. 264:296
- Marscher et al. 1979,Ap.J. 233:498
- Miley 1980,Ann. Rev. A.& A. 18:165
- Moore & Stockman 1984,Ap.J. 279:465
- Pauliny-Toth et al. 1981,Astr.J. 86:371

- Pearson & Readhead 1981,Ap.J. 248:61
- Phinney 1983,Ph.D. thesis,Cambridge University
- Pringle 1981,Ann. Rev. A.& A. 19:137
- Rees 1967,MNRAS 135:345
- Rees 1971,Nature 229:312,510
- Rees 1984,Ann. Rev. A.& A. 22:471
- Rees 1984,Proceedings of the Conference:"X-ray and UV emission from AGNs", MDE report
- Rees,Begelman,Blandford & Phinney 1982,Nature 295:17
- Robson et al. 1983,Nature 305:194
- Rybicki & Lightman 1979, Radiative Processes in Astrophysics (Wiley,New York)
- Serabyn & Lacy 1985,Ap.J. 293:445
- Shapiro & Lightman 1976,Nature 315:743
- Shapiro & Teukolski 1985,preprint
- Shields 1978,Nature 272:706
- Shields & Wheeler 1978,Ap.J. 222:667
- Sikora 1981,MNRAS 196:257
- Stein,O'Dell & Strittmatter 1976,Ann. Rev. A.& A. 14:173
- Stockman,Moore & Angel 1984,Ap.J. 279:485
- Svensson 1984,Proceedings of the Conference:"X-ray and UV emission from AGNs",MDE report
- Ulrich et al. 1984,MNRAS 206:221
- Unwin et al. 1985,Ap.J. 289:109
- Urry & Mushotzy 1982,Ap.J. 253:38
- Wandel 1985,in "Trieste meeting on structure and evolution of AGNs",in press
- Weiler & Johston 1980,MNRAS 190:269
- Wiita 1985,Physics Reports 123:117
- Worrall et al. 1982,Ap.J. 261:403
- Young et al. 1978, Ap.J. 221:721
- Zamorani et al. 1981,Ap.J. 245:357
- Zensus,Porcas & Pauliny-Toth 1984,Astron. Astrophys. 133:27